CORTEX

Research and Innovation Action (RIA)

This project has received funding from the European Union's Horizon 2020 research and innovation programme under grant agreement No 754316.

Start date : 2017-09-01 Duration : 48 Months
http://cortex-h2020.eu

Experimental report of the 3rd campaign at AKR-2 and CROCUS

Authors : Dr. Vincent LAMIRAND (EPFL), Alexander KNOSPE (TUD), Klemen AMBROZIC (EPFL), Fanny VITULLO (EPFL), Carsten LANGE (TUD),

CORTEX - Contract Number: 754316

Project officer: Marco Carbini

Document title	Experimental report of the 3rd campaign at AKR-2 and CROCUS
Author(s)	Dr. Vincent LAMIRAND, Alexander KNOSPE (TUD), Klemen AMBROZIC (EPFL), Fanny VITULLO (EPFL), Carsten LANGE (TUD),
Number of pages	36
Document type	Deliverable
Work Package	WP02
Document number	D2.4
Issued by	EPFL
Date of completion	2021-08-30 17:29:40
Dissemination level	Public

Summary

In the framework of the CORTEX project, the work package 2 targets the generation of high quality neutron noise experimental data for the subsequent validation of computer methods and models developed in work package 1. The AKR-2 reactor at TUD, and the CROCUS reactor at EPFL, are the experimental facilities where noise-specific experimental data are being generated. This report documents the setup and experiments for each perturbation type and facility of the third campaigns. The raw time series were already distributed to the members of the consortium. The associated experimental results will be documented in separate internal reports and distributed to the members of the consortium.

Approval

Date	By
2021-08-31 08:36:19	Mr. Mathieu HURSIN (EPFL)
2021-08-31 08:38:17	Pr. Christophe DEMAZIERE (Chalmers)

Table of contents

Index of Tables

Index of Figures

Abbreviations

AC	Alternating Current
AVS	Absorber of Variable Strength
BB	Beagle-Bone
BNC	Bayonet Neill–Concelman connector
CIC	Compensated Ionization Chamber
COLIBRI	CROCUS Oscillator for Lateral Increase Between u-metal Rods and Inner zone
DAQ	Data acquisition system
DC	Direct Current
ECCP	Electronic Collaborative Content Platform
EPFL	Ecole Polytechnique Fédérale de Lausanne
FC	Fission chamber
FFM	Fix Filter Module
FFT	Fast Fourier Transform
FPGA	Field-Programmable Gate Array
ISTec	TÜV Rheinland ISTec GmbH – Institut für Sicherheitstechnologie
MFC	Miniature Fission Chamber
MCS	Multi-Channel Scaler
PC	Proportional Counter
PE	Polyethylene
PMMA	Poly (methyl methacrylate)
PRM1	linear Power-Range channel Monitor 1
PSD	Power Spectral Density
SAD	Simultaneous Analog-Digital converter
SiPM	Silicon Photomultiplier
TTL	Transistor-Transistor Logic
TUD	Technische Universität Dresden
U_{metal}	Metallic uranium
UO_2	Uranium oxide
VA	Vibrating Absorber
WP	Work package
WRM	Wide-Range channels Monitor (WRM1 and WRM2)

Summary

In the framework of the CORTEX project, the work package 2 targets the generation of high quality neutron noise experimental data for the subsequent validation of computer methods and models developed in work package 1. The AKR-2 reactor at TUD, and the CROCUS reactor at EPFL, are the experimental facilities where noise-specific experimental data are being generated. This report documents the experimental setup and measurements for each perturbation type and facility of the third campaigns. The raw time series were already distributed to the members of the consortium. The associated experimental results will be documented in separate internal reports and distributed to the members of the consortium.

1 Overview

The CORTEX project aims at developing an innovative core monitoring technique for anomaly detection in nuclear reactors, such as excessive vibrations of core internals, flow blockage, coolant inlet perturbations, etc. The technique will be based on primarily using the inherent fluctuations in neutron flux recorded by in-core and ex-core instrumentation, from which the anomalies will be differentiated depending on their type, location and characteristics. The method is non-intrusive and does not require any external perturbation of the system. The project will result in a deepened understanding of the physical processes involved. This will allow utilities to detect operational problems at a very early stage and to take proper actions before such problems have any adverse effect on plant safety and reliability.

The main purpose of the experimental campaigns at the AKR-2 and CROCUS reactors is to produce high quality noise-specific experimental data for the validation of the neutron noise computational models. The first and second campaigns were presented in [1]–[3]. The present document is dedicated to the third campaigns, and is structured in two main sections: a first one describing the third experimental campaign at the AKR-2 reactor, and a second one describing the third experimental campaign at the CROCUS reactor. Along this report, all experimental data are distributed to all partners in the form of time series identified by their measurement number, instrumentation, and signal's number.

For the 3rd experimental campaign at the AKR-2 at the TU Dresden, 46 experiments were performed. The same two perturbation devices were used: an absorber of variable strength and a vibrating absorber, used either separately or together. The reactor response was recorded via 7 detectors: 5 He-3 proportional counters, and 2 fission chambers closer to the core. Compared to the second campaign, the motion of the perturbations was recorded for both devices with digital position trigger signals, and additionally with an analogue signal for the linear motion of the vibrating absorber. All detector signals were acquired with a Zynq FPGA board with 8 possible TTL input for synchronization purposes.

At CROCUS at EPFL, the 3rd experimental campaign focused on the repetition of one specific case of fuel rods oscillation (±1.5 mm, 1 Hz) for repeatability purposes, and the enhancement of the spatial dependence of noise using a second oscillator, namely the POLLEN vibrating absorber. COLIBRI and POLLEN perturbation devices were applied separately and together (in synchronization), always at 1 Hz frequency for comparison purposes. 38 experiments were carried out in total, which were measured using 18 detectors distributed within and around the core, as well as at distance in the fast neutron energy range. The three additional detectors as compared to the second campaign consisted in miniature neutron scintillators [4]. Two were set close to the perturbations, and a last one was set in a device allowing for observing the angular dependence of the neutron flux. Static experiments were conducted for detectors and criticality reference values.

Although a large part of the experimental setups were already detailed in the previous reports, all details are stated here again for the sake of completeness of the report at hand. Reactor characteristics and configurations are unchanged. Changes in setup with respect to the second campaigns are indicated. The changes concern mainly the detectors' setup, a general improvement of signal acquisition, and the addition of a perturbation for CROCUS.

2 AKR-2 third experimental campaign

The third experimental campaign at AKR-2 took place between 22nd February 2021 and 26 February 2021, with additional experiments from 4th March 2021 to 10th March 2021. Two perturbation devices were used as noise sources: a rotating absorber which acts as an absorber of variable strength, and a linearly oscillating absorber acting as vibrating absorber. The motion of the perturbations was recorded for both devices with digital position signals, triggering at a specific state of the motion. In addition, the linear motion of the vibrating absorber was recorded, producing an analogue signal. Five He-3 proportional counters and two fission chambers were used to measure the neutron noise signals. These signals were acquired with a Zynq FPGA board with 8 possible TTL input and an additional minicomputer BeagleBone Black.

46 experiments with known perturbations were conducted in total. 12 of these experiments were performed with the absorber of variable strength, 25 experiments with the vibrating absorber, and 9 experiments with both perturbations running at the same time.

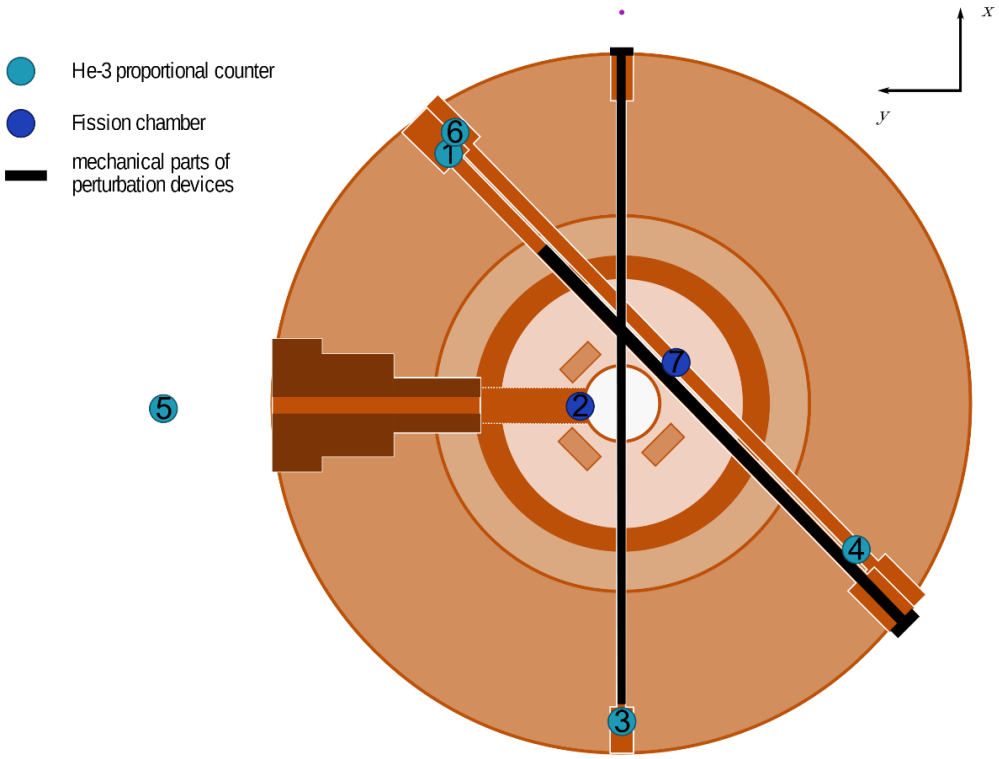

Figure 1 – Schematic overview of the detector setup and the location of the perturbation devices of the 3rd measurement campaign at AKR-2.

2.1 The AKR-2 reactor

The AKR-2 reactor, located at TU Dresden, is a thermal, zero-power reactor with an allowed maximum thermal operation power of 2 W. The core has cylindrical shape with a diameter of 250 mm and a height of 275 mm. The disk-shaped fuel elements consist of a homogeneous dispersion of polyethylene moderator and uranium oxide, which is enriched to 19.8 %. For security reasons the core is separable, with the lower half being movable. For the basic start-up procedure, the core halves are brought together. The operation is controlled by three control and safety rods installed next to the fuel zone, consisting of cadmium sheets on polyethylene blocks. A graphite reflector with approx. thickness of 32 cm surrounds the core. Underneath and above the core is about 25 cm and 70 cm graphite, respectively. The biological shield consists of two cylindrical walls of 15 cm and 58 cm thickness, made of paraffin and heavy concrete. The reactor is accessible via seven horizontal and two vertical experimental channels. The setup of AKR-2 is illustrated in Figure 2. The tall central channel 7 was, again, partially filled with polyethylene-elements, leaving just a cylindrically shaped hole with a diameter of 13 cm in the cylindrical part of the channel (see Figure 1).

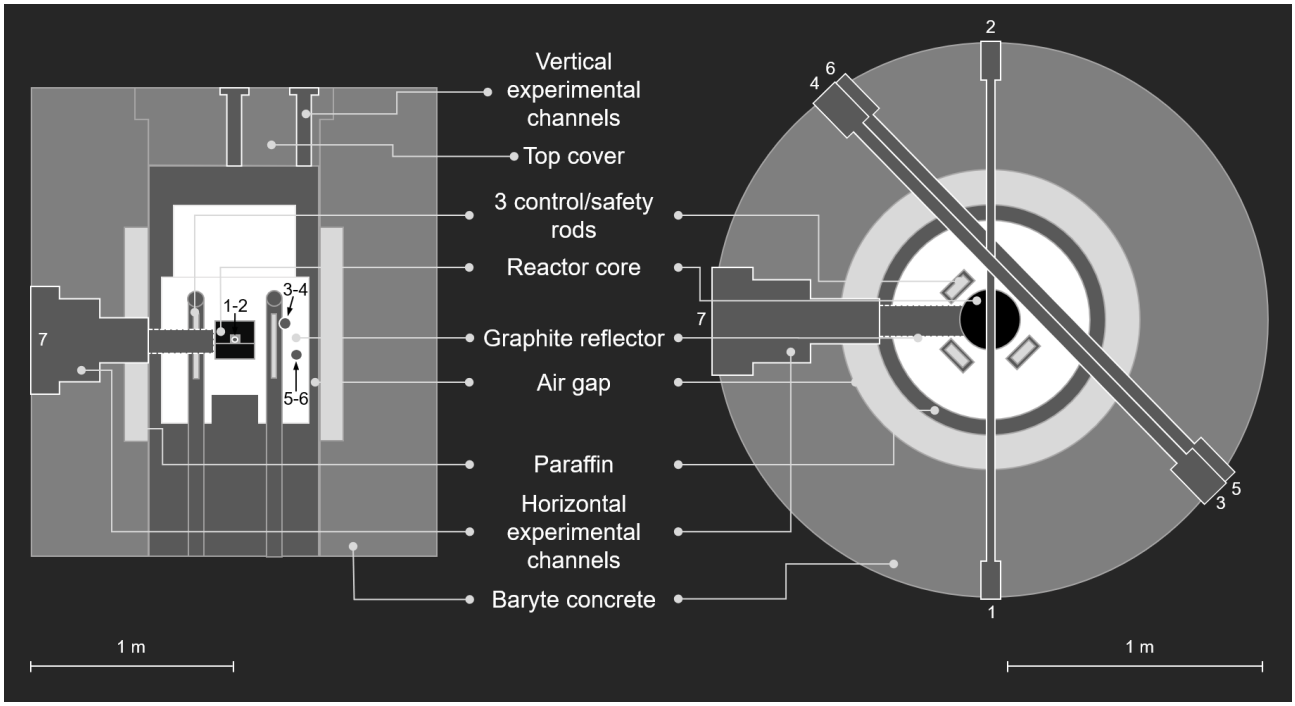

Figure 2 – Schematic of the AKR-2 reactor.

2.2 Perturbation devices

During the third campaign, the same two perturbation devices were used as in the second campaign. One of them is a rotating cadmium absorber which was inserted into channel 3-4 and which is driven by a stepper motor. The second one is an aluminium rod with an indium absorber inside, driven by a linear motor axis. They act as absorber of variable strength and vibrating absorber, respectively. With respect to the 2nd measurement campaign at AKR-2, only the driving mechanism of the absorber of variable strength was updated. The vibrating absorber remains unchanged.

2.2.1 Vibrating absorber

The vibrating absorber produces a sine motion of the absorber along channel 1-2 which introduces a periodic perturbation in the reactor. To this end an aluminium shaft containing an indium absorber is inserted into the experimental channel 1-2. The absorber is a stack of 13 indium foils with a diameter of 12.7 mm. The cumulative mass of indium is 926.2 mg. It consists of high purity natural indium. The linear axis can be driven with different motion profiles. A sine motion with different amplitudes and frequency was selected for this measurement campaign. The principle of the setup is shown in Figure 3. The axis position is given by its internal reference. This means that the core centre is at 10.5 cm and the axis is driving towards the channel exit 2 for higher numbers of this internal position.

The position of the axis is recorded in two different ways. Firstly, a digital position signal indicates either when the oscillation reaches its turning point for 0.1 Hz or lower frequencies, or if the axis moves out of the reactor for frequencies above. Additionally, the position is recorded continuously via a motion encoder with an analogue input pin on a BeagleBone Black minicomputer.

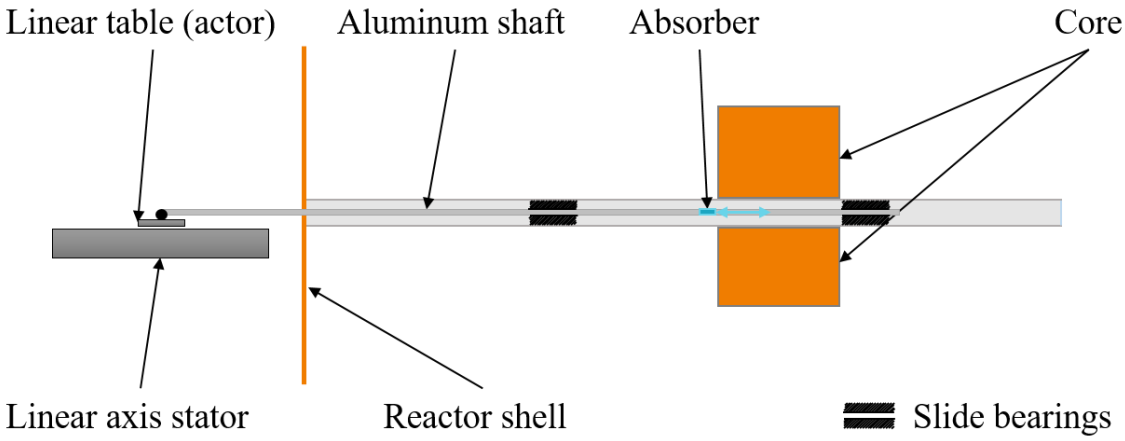

Figure 3 – Schematic of the vibrating absorber.

2.2.2 Absorber of variable strength

The absorber of variable strength inserts a localized perturbation. For the 3rd CORTEX campaign, it is realized by an absorber, rotating in the experimental channel 3-4, driven by a stepper motor, where the stepper motor was upgraded to allow for higher frequencies. The absorber is a bent rectangular cadmium sheet with dimensions of 25 cm x 2 cm x 0.02 cm with a bending and rotation radius of 2.98 cm. The largest dimension is parallel to the experimental channel. The material of the absorber is natural cadmium with unknown impurities.

The absorber is driven with a constant angular velocity in clockwise direction. This motion is recorded with an inductive sensor which is located at the 9 o'clock position as seen from channel opening 3 which produces a high when the absorber passes this position. This setup is illustrated in Figure 4.

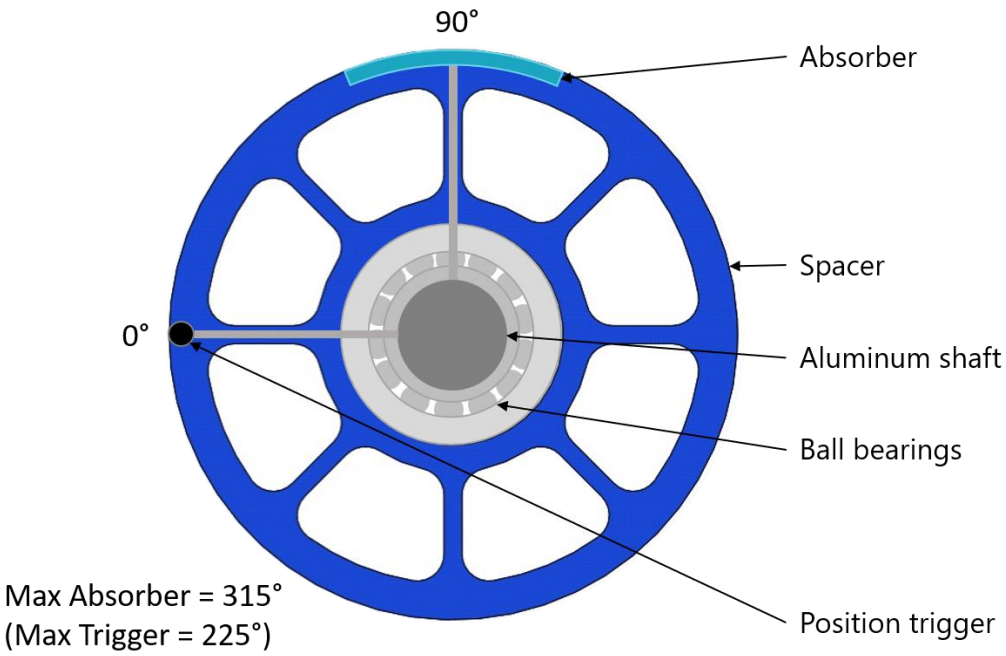

Figure 4 – Schematic of the absorber of variable strength.

2.3 Neutron detection instrumentation

During the 3rd measurement campaign at AKR-2 seven detectors were used, 5 He-3 proportional counters and 2 fission chambers closer to the core. All these detectors were inserted into experimental channels inside the AKR-2 reactor. The approximate location of the detectors and how they were connected to the AKR-2 DAQ systems can be seen in Figure 5. Switches indicate that the input is used for different signals, depending on the experiment. Changes with respect to the 2nd campaign are indicated, and mainly concern the detectors setup for modelling purposes. In addition, signals synchronization was achieved by using only one Zynq FPGA acquisition board for all detector's signals, and a binary position signal for each perturbation (new for the vibrating absorber).

2.3.1 Detectors

For the detection of the reactor's response to the perturbations, seven different detectors were used. Two of them were fission chambers (2, 7) and the other five were He-3 proportional counters (1,3,4,5). The exact position of the detectors can be seen in Table 1.

With respect to the 2nd campaign, the detector locations and numberings were changed (see Table 1 for the exact locations and types). Detector locations of detectors 1 and 4 roughly correspond to 5 and 1 of the second campaign. Detector 7 was used to compensate for the lack of detectors 7, 8 and 9 of the second campaign. Detector 5 was added as a monitor of detector 2. Detectors 2, 3 and 6 are roughly, but not exactly, at the same location as in the second campaign. None of the permanently installed detectors were used for the 3rd experimental campaign at AKR-2.

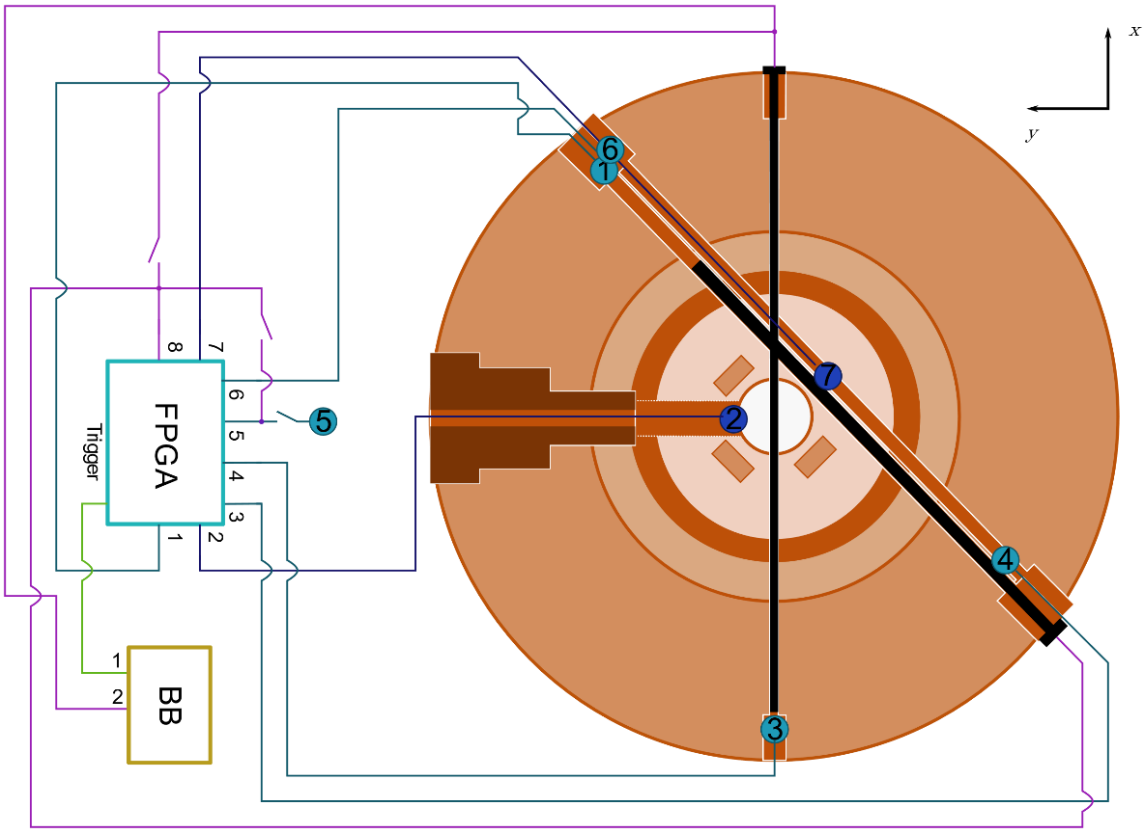

Figure 5 – Schematic of the detector locations in the 3rd AKR-2 measurement campaign.

Table 1 – Detectors for the 3rd experimental campaign at AKR-2. (0,0,0) is center of the reactor mid-channel 1-2, x along channel 1-2, y along channel 7. All dimensions are in cm.

No	Type	Sensitive material	Dimensions		Position			
			Diameter	Active length	Orientation	x	y	z
1	PC	^{3}He gas	2.42	20	(-1,-1,0)	89	57.9	8
2	FC	^{235}U deposit				0	16.8	0
3	PC	^{3}He gas	2.42	20	(1,0,0)	-114.97	0	0
4	PC	^{3}He gas	2.42	20	(1,1,0)	-47.5	-89.9	-8
5	PC	^{3}He gas	2.42	20	(1,0,0)	0	166.7	0
6	PC	^{3}He gas	2.42	20	(-1,-1,0)	90.6	48.2	-8
7	FC	^{235}U deposit				21.21	-21.21	-8

2.3.2 Data acquisition systems

The data acquisition system for the 3rd measurement campaign at AKR-2 was simplified by using only a Zynq FPGA board for the neutron detection system in order to achieve synchronization between the signals. The raw signal of the FPGA is provided as a sequence of binary file containing the time difference between consecutive neutron detection events in number of FPGA clock cycles (10 ns) as unsigned 32 bit integer. These files have been converted into a standardized text file and are available on the Cortex ftp at this address:

`/export/zh4/cortex/tud/Data_3rd_Campaign/`

Both the linear motor axis and the rotating absorber provided a binary signal to allow for synchronization during post-processing of the data. The rotating absorber signal produces a high if the rotating absorber is at the 9 o'clock position. The linear axis signal is high either at the turning point of the oscillation or if the absorber moves out of the channel. Which mode is used depends on the frequency of the oscillation and is specified in Table 6 in Appendix 6.2 (p. 27). For measurements with both perturbations running simultaneously the position signals are on input sensor 5 and 8 of the FPGA, otherwise the position signal is on sensor 8.

Furthermore, the axis position signal is recorded via a relative motion encoder as voltage on a BeagleBone Black minicomputer. This minicomputer records Unix time-stamps together with the voltage of the motion encoder and the trigger signal as 12-bit unsigned integers. This position signal was converted to the standardized ASCII format.

2.3.2.1 FPGA board

The FPGA-board has 8 BNC inputs for the acquisition of TTL-pulses. Additionally, there are trigger-in and trigger-out channels. The detector signals are connected to the inputs according to their detector number. The digital position signal is generally recorded at input number 8. For measurements with both perturbation devices operating at the same time detector number 5 was disconnected and input signal 5 recorded the digital position signal of the absorber of variable strength. Due to a mix-up in the input cables, detectors 1 and 6 are switched for measurements in March. That means that for measurements with designations M33 and higher input signal 1 is actually detector 6 and the other way around. This mix-up was fixed in post-processing.

The raw signals are saved in 32 bit binary files containing the differences between individual neutron detection events in multiples of clock cycles of the FPGA (10 ns). All raw data files have also been converted to a standardized .txt files (see section 2.3.3).

2.3.2.2 Beagle-Bone

The mini-computer BeagleBone Black is able to acquire analogue signals. It is used to acquire the signal of the linear motion encoder for the vibrating absorber. The voltage level of the motion encoder signal was manually adjusted for every measurement to provide the maximum possible bit depth. The signal is stored in an ASCII file containing the timestamp in the first column, the trigger level in the second column and the motion signal in the third column.

2.3.3 Standardized txt file format

All raw data was converted to a standardized txt file format in form of a time series (an example is depicted in Figure 6). The first line of the txt file contains a header with relevant information. Line 2 contains the dwell time followed by the detector signals. Due to interpolation of the signals or the analogue nature of the Beagle-Bone signal, the detector values are floating point numbers.

The data can be found on the Chalmers ftp server in the folder:

`/export/zh4/cortex/tud/Data_3rd_Campaign/txt_data`

The files have the following naming convention:

`AKR2_experiment number_data acquisition system_detector number.txt`

The data acquisition systems are MCS, BB, FPGA, EPFL, FPGA-pos and BB-pos, where the last two refer to position signal and are assigned detector numbers 10 and 11.

```
# AKR-2 - det_01 - MCS - Measurement # 1 - Power (W) 1.5 - tw (s) 0.04 - tm (s) 2621.36 - expfreq (Hz) 2.0 - First value below corresponds to the dwell time (s)
0.04000
154.00000
168.00000
173.00000
172.00000
188.00000
135.00000
164.00000
170.00000
181.00000
179.00000
186.00000
187.00000
174.00000
162.00000
177.00000
181.00000
```

Figure 6 – Example of the standardized txt format provided for the time series.

2.4 Experiments

Table 2 shows the conducted noise experiments. The complete and detailed list of experiments is in appendix 6.2 (p. 27). For the measurement M07, the position signal was faulty. This measurement should not be used. As mentioned above, for measurements M33 upwards, detector input signals on the FPGA were switched for detectors 1 and 6.

Table 2 – List of experiments at AKR-2.

Designation	Type	Frequency (Hz)	Center position (cm)	Amplitude (cm)	Measurement duration (s)
M01	AVS	0.1	N.A.	N.A.	2000
M02	AVS	2	N.A.	N.A.	2000
M03	AVS	10	N.A.	N.A.	2000
M04	VA	2	14.5	0.5	2000
M05	VA	10	14.5	0.5	2000
M06	VA	0.1	14.5	0.5	2000
M07	VA	0.1	14.5	0.5	2000
M08	VA	0.1	14.5	0.5	2000
M09	VA	2	14.5	0.5	2000
M10	VA	10	14.5	0.5	2000
M11	AVS	0.1	N.A.	N.A.	2000
M12	AVS	2	N.A.	N.A.	2000
M13	AVS	10	N.A.	N.A.	2000
M14	VA	1	10.5	2	2000
M15	VA	0.1	10.5	3	2000
M16	VA	2	10.5	3	2000
M17	VA	2	16	3	2000
M18	VA	0.1	16	3	2000
M19	VA	1	10.5	2	2000
M20	VA	0.1	10.5	3	2000
M21	VA	2	10.5	3	2000
M22	Both	2	14.5	0.5	2000
M23	Both	0.1	14.5	0.5	2000
M24	Both	2	16	3	2000
M25	VA	2	14.5	0.5	2000
M26	Both	2	14.5	0.5	2000
M27	Both	0.1	14.5	0.5	2000
M28	Both	2	16	3	2000
M29	VA	2	16	3	2000
M30	VA	0.1	16	3	2000
M31	AVS	4	N.A.	N.A.	2000
M32	AVS	4	N.A.	N.A.	2000
M33	AVS	10	N.A.	N.A.	2000
M34	AVS	2	N.A.	N.A.	2000
M35	AVS	0.1	N.A.	N.A.	2000
M36	VA	2	14.5	0.5	2000
M37	VA	10	14.5	0.5	2000
M38	VA	0.1	14.5	0.5	2000
M39	VA	1	10.5	2	2000
M40	VA	2	10.5	3	2000
M41	VA	0.1	10.5	3	2000
M42	Both	2	14.5	0.5	2000
M43	Both	0.1	14.5	0.5	2000
M44	Both	2	16	3	2000
M45	AVS	4	N.A.	N.A.	2000
M46	VA	2	16	3	2000

3 CROCUS third experimental campaign

The third experimental campaign in the CROCUS reactor took place from 4th to 17th March 2021. The reactor configuration is unchanged as compared to previous campaigns. However, two perturbation devices were used in this campaign:

- The COLIBRI fuel rods oscillator (CROCUS Oscillator for Lateral Increase Between u-metal Rods and Inner zone): an in-core device that was specifically developed for the investigation of fuel rods vibration within the namesake program in CROCUS, and which was already used in previous campaigns,
- The POLLEN vibrating absorber (Pile Oscillator for Localized and Low Effect Noise): new perturbation device which allows the axial oscillatory movement of a cadmium absorber sample within a guide tube. It is designed to be operated in synchronization with COLIBRI.

The basic detector setup remained relatively similar as for the second campaign, with the addition of three detectors based on miniature scintillators coupled to optical fibers:

- A detector located on the transmission beam of COLIBRI,
- A detector located on the experimental channel of POLLEN,
- A detector enveloped in an iris made of cadmium, for observing the angular dependence of the neutron noise.

38 experiments were carried out in total. This section describes the CROCUS reactor, both the COLIBRI and POLLEN perturbation devices, the detectors and data acquisition setup, and finally the conducted experiments.

3.1 The CROCUS reactor

CROCUS is an experimental zero-power reactor, uranium-fueled and water-moderated, dedicated to teaching radiation and reactor physics, and to research. It is located at the École Polytechnique Fédérale de Lausanne (EPFL) and it has been licensed for operating at a maximum power of 100 W, i.e. a total neutron flux of ~2.5×10^9 n/cm^2/s at the core center. Criticality is controlled either by changing the core's water level using a spillway, or by two B_4C absorber control rods, with an accuracy of ±0.1 mm (equivalent to approximately ±0.4 pcm) and ±0.5 mm, respectively. CROCUS operates at room temperature using a controlled water loop with secondary and tertiary circuits, two heat exchangers and an electrical heater.

The core is located in an aluminum vessel of 130 cm in diameter and 1.2 cm in thickness. It is filled with demineralized light water, acting as both moderator and reflector. Its active part has the approximate shape of a cylinder of about 60 cm in diameter and 1 m in height. It consists of two interlocked fuel zones with square lattices of different pitches: an inner zone of 336 UO_2 rods with an enrichment of 1.806 wt.% and a pitch of 1.837 cm; an outer zone of 172 U_{metal} rods in nominal configuration, 0.947 wt.% and 2.917 cm pitch; a varying water gap between the two zones because of the two different pitches. The picture of the facility and critical assembly configuration is shown in Figure 7. Both uranium fuels consist of a 1-m pile of cylindrical pellets cladded in aluminum. The rods are maintained vertically by two octagonal aluminum grid plates spaced 1 m apart. The grids have a 0.5-mm cadmium layer to limit axial neutron leakage to the environment, i.e. structures activation, with the active zone of the fuel starting above the lower cadmium layer.

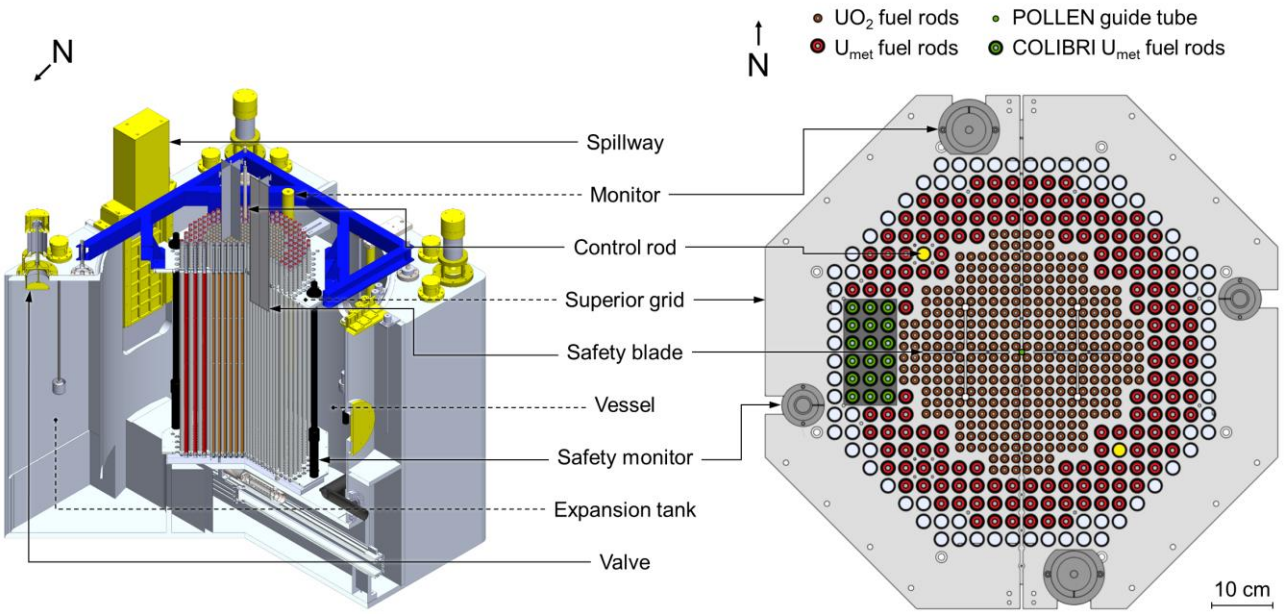

(a) Core structure and internals, isometric view (b) Upper grid and fuel lattice

Figure 7 – The CROCUS reactor: isometric view of the vessel (left), and top view of the core superior grid and configuration, with the indication of the location of the COLIBRI and POLLEN perturbation devices, in the West region and core centre, respectively (green).

3.2 Perturbation devices

During the 3rd campaign in CROCUS, two perturbation devices are employed, separately or together in synchronization. They consist of the COLIBRI fuel rods oscillator, which is unchanged with respect to previous campaigns, and the POLLEN vibrating absorber. Both are presented hereafter.

3.2.1 The COLIBRI fuel rods oscillator

The COLIBRI fuel rods oscillator is designed to simultaneously oscillate up to 18 metallic uranium fuel rods laterally in the west region of the core periphery zone. It consists in two moving plates set above and below the core grids, rigidly connected by an aluminum beam (see Figure 8). Each one carries an extremity of the fuel rods, top and bottom respectively.

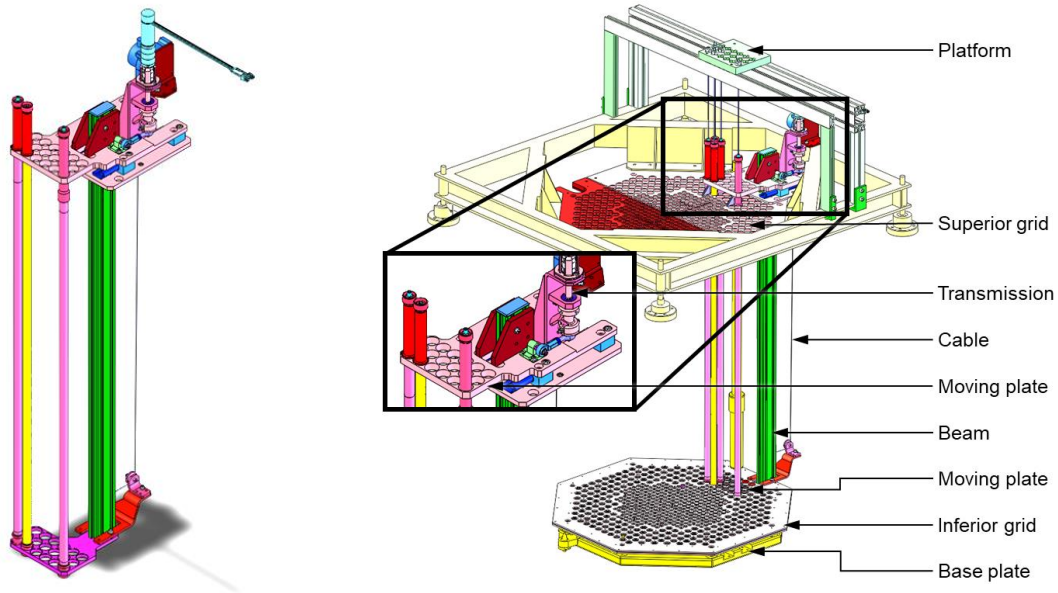

Figure 8 – COLIBRI fuel rods oscillator with a few fuel rods inserted in the device, alone (left) and with core structures (right).

The top moving plate is fixed on the superior grid *via* gliders. Its oscillation is produced by a stepper motor: the motor rotation is converted to a linear translation using an eccentric sheave and a connecting rod. The oscillation is transferred to the bottom moving plate *via* the aluminum beam. The bottom moving plate is free of movement except for the connection to the transmission beam (no gliders).

New grids were produced to accommodate the oscillator. Aside from the enlarged holes at COLIBRI's location, the cadmium layer sandwiched in each grid was increased to from previous 0.5 mm to 1 mm thickness (see Figure 9 and Figure 10). Other mechanical parts, located far in the reflector, or above and below the grids, are not detailed in this document as they are not relevant for the modeling.

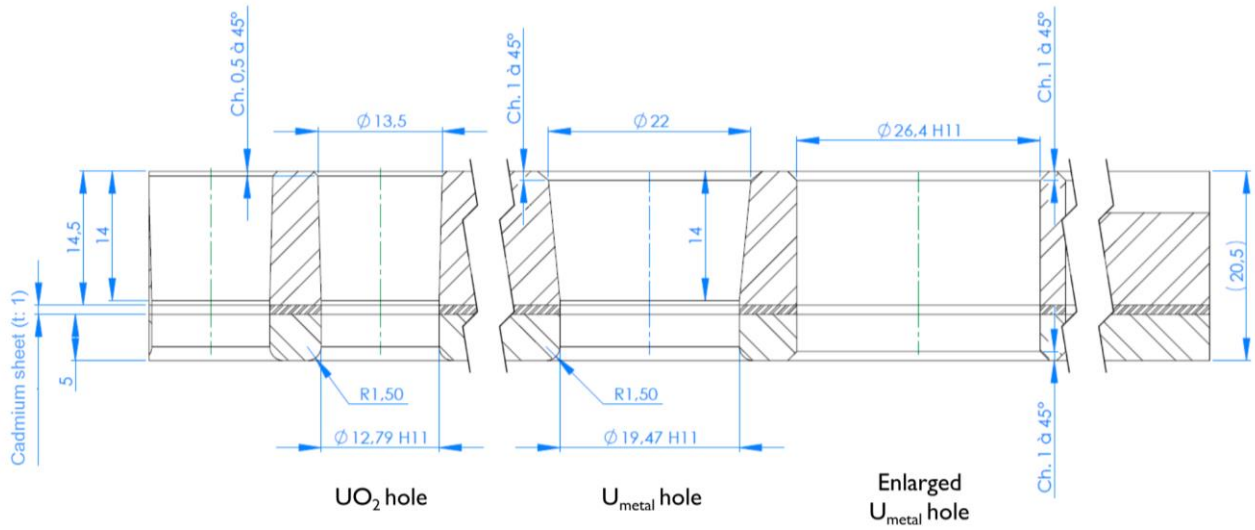

Figure 9 – Cross section of the modified superior grid: enlarged holes in COLIBRI's region and thicker cadmium layer (1 mm).

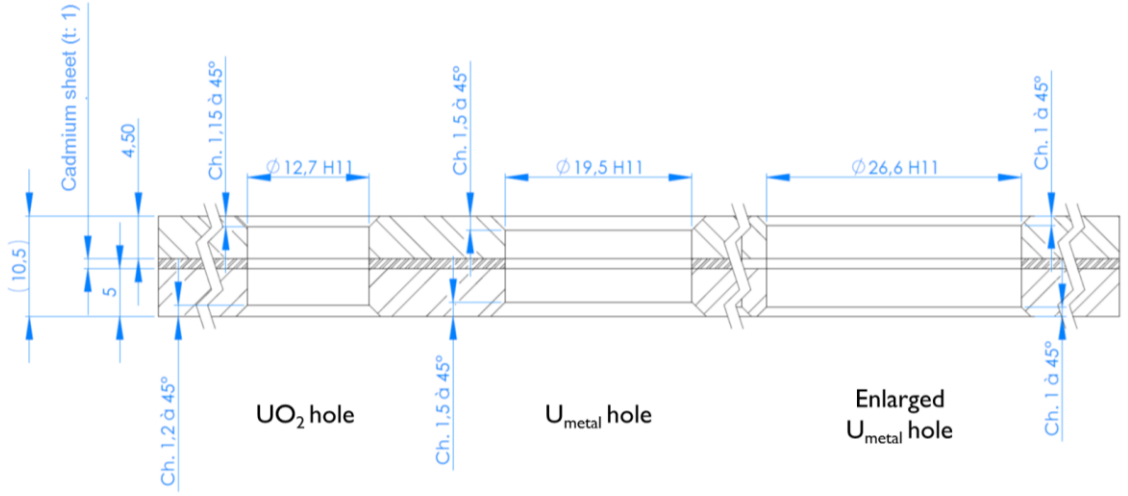

Figure 10 – Cross section of the modified inferior grid: enlarged holes in COLIBRI's region and thicker cadmium layer (1 mm).

The selection of the moving fuel rods is performed by leaving them laying on the reactor base plate (non-moving), or suspending them up 10 mm above the base plate to insert them in the moving plates. Top and bottom end caps are fixed to each rod to allow for the insertion in the enlarged holes of either the static grids or the moving plates (see Figure 11). The weight of the oscillating rods is supported by a platform. The amplitude of the oscillation is precisely tuned by changing the eccentricity of the sheave with calibration plates, 0.5 mm by 0.5 mm from 0 to ±2.5 mm. Its frequency is depending on the speed of the motor, with a fixed conversion factor.

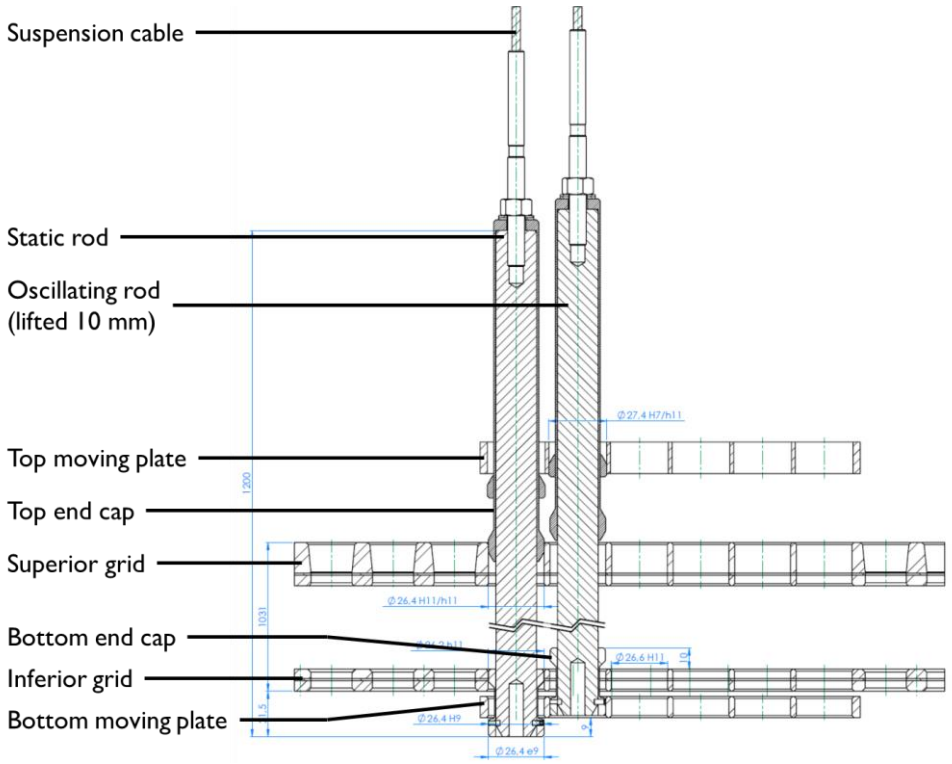

Figure 11 – Side cross section of the oscillator with only two fuel rods inserted in it; one fuel rod is in its static configuration laying at the bottom (left), the other one is lifted up 10 mm for oscillation.

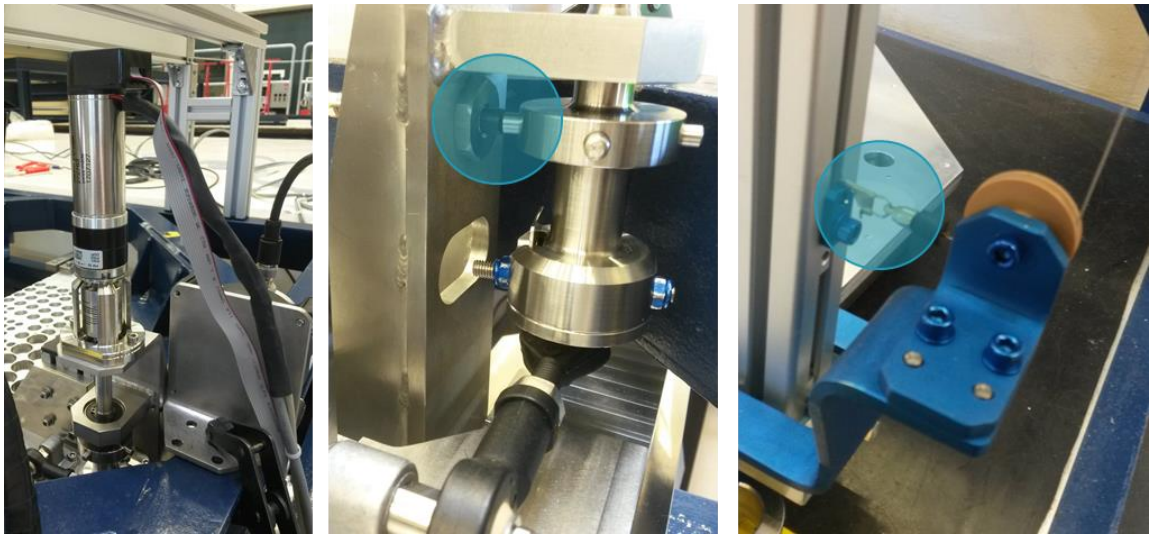

Figure 12 – Details of the control and monitors of the oscillation: (left) Motor on its rotation axis; (center) Close-up on the rotation axis with focus (blue) on the inductive captor detecting one of the four pins; (right) Measuring cable and close-up (blue) on its connection at the bottom to the transmission aluminum beam.

The oscillation is controlled and monitored *via* a LabVIEW-based software. An inductive captor is set at the rotation axis (i.e. at the top), which detects the actual movement of the motor by detecting the passage of four metallic pins per rotation, one being slightly larger for identification purposes. A cable coder is used to measure the displacement of the moving plate, i.e. at the bottom, with a 0.1 mm precision. These features are presented in Figure 12. The software generates as a csv file output the recording of the motor position and speed, the signal of the inductive captor, and the measurement of the cable length, with 10 ms time-steps. A typical recording of an oscillation is

presented in Figure 13. The inductive captor signal output is also extracted for recording using the detection instrumentation (allowing signal synchronization), and direct use (e.g. for POLLEN).

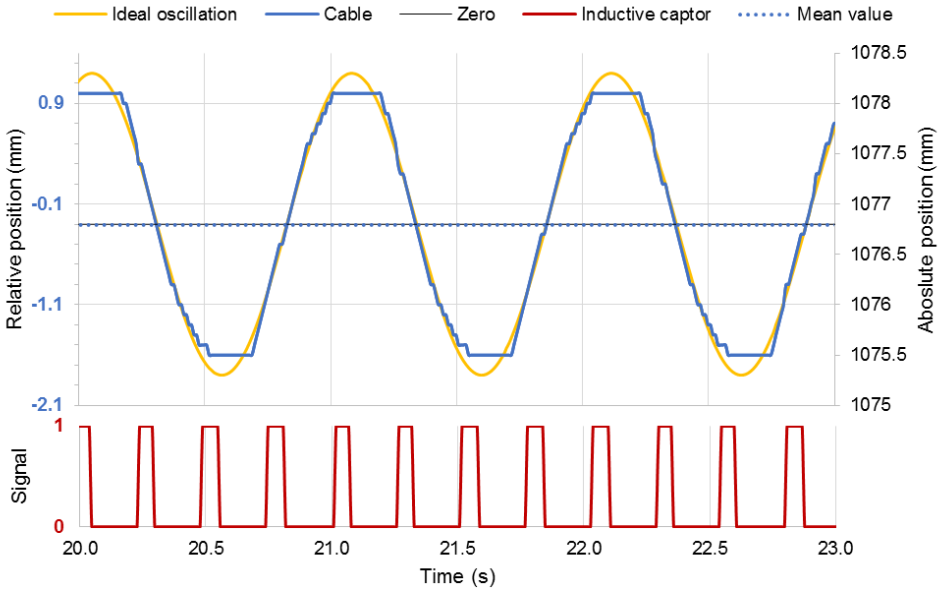

Figure 13 – Typical inductive captor (bottom, red) and cable (top, blue) signals, here in the case of one rod oscillating in air at ±1.5 mm and 1 Hz. In yellow, ideal sinusoidal oscillation for comparison with the real and measured displacement. The mean of the signal and the zero, which corresponds to the rods' nominal position, are also represented.

The behavior of the oscillator has been characterized in air and in water, out of the vessel and in-core, and with different loads: empty, one rod, and 18 rods (i.e. fully loaded). The behavior in frequency is sound. In amplitude, the device is rigid at the top, depending only on the rotation to translation conversion: a 0.1 mm flattening of the sinusoid due to mechanical plays in the crank and rod is expected (see Figure 13). Results on the oscillation amplitude at the bottom are presented in Figure 14. It demonstrates inertia effects inducing an increase of the amplitude for the full 18-rods load case above 1 Hz, which is the case of the measurement campaign described in this report. This effect cannot be corrected, and thus has to be taken into account as is.

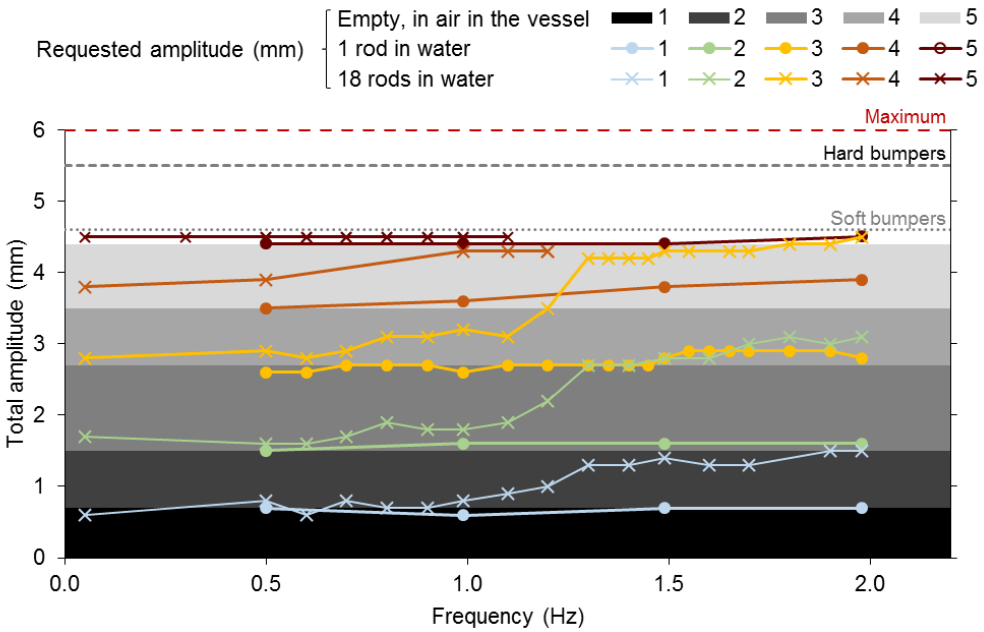

Figure 14 – Comparison of the oscillator behavior measured at the bottom position for 1 and 18 rods loads (connected dots and crosses, respectively) in water (1000 mm level). Behavior of the device when oscillating empty loaded in air is shown as well (grey bars), for reference as it is expected to be equivalent to the behavior of the top part. All measurements were carried out using the cable coder.

3.2.2 The POLLEN vibrating absorber

Aside allowing complementary vibrating absorber experiments in CROCUS, the POLLEN oscillator was designed to compensate the reactivity change induced by COLIBRI, and as such maximize the spatial dependence of noise. It consists of an absorber (7 mm-outer diameter) made of a Cd piece (8.1 cm-long, 1 mm-thick) rolled on a thin PMMA rod, suspended into an in-core aluminium guide tube (10 mm-outer diameter, see Figure 15, left). The guide tube is set at the central axis of the core, and lies on the reactor base plate. It is maintained in its vertical position by a PMMA fixation piece screwed to the adjacent fuel rods. The sample radial position in the core is determined by the central position of the guide tube, while its axial position is controlled by a pulley, connected to a geared stepper motor. The motor is controlled via a stepper motor driver and a National Instruments (NI) controller (Figure 15, right), operated using a custom LabView software.

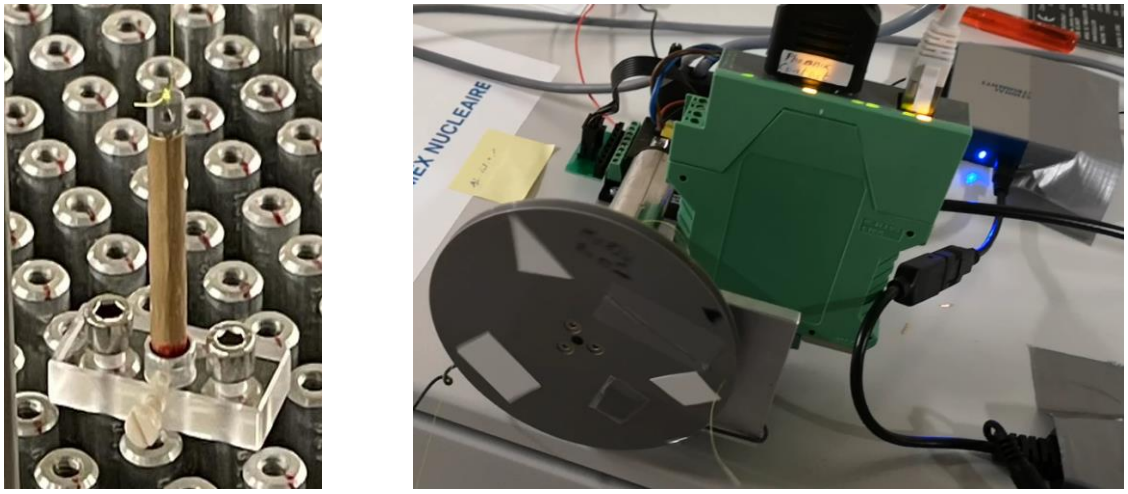

Figure 15 – On the left, Cd absorber sample of POLLEN, half inserted in its aluminium guide tube in the core centre. The red line denotes the absorber mid-height. On the right, POLLEN pulley (grey disk) connected to a geared stepper motor, a driver (in green), and an NI controller (in grey with the blue LED on) during out-of-pile tests.

The software is used to set up the stationary position of the motor and absorber, as well as to induce a periodic oscillation. The oscillation is governed in time by the inductive captor signal from COLIBRI in order to allow the synchronization of the two perturbations. From extensive testing, a lag of 0.64 s was observed between inductive captor signal and the NI controller triggering the POLLEN oscillator, which was taken into account for the campaign. It was observed during the campaign that POLLEN could erroneously shift its 800 mm nominal position because of a programming issue. Unfortunately, it impacts the reactivity worth (mainly in amplitude), and it will have to be considered in the interpretation of the results.

Some experiments were performed with both COLIBRI and POLLEN, while some were performed with POLLEN alone. Due to the fact that the POLLEN oscillations are governed by the COLIBRI inductive captor signal, POLLEN only operation was realized by setting the COLIBRI oscillation amplitude to 0 using the appropriate plate: COLIBRI's motor and axis were turning and thus feeding POLLEN, without inducing any fuel rods oscillation.

The induced oscillation is defined in amplitude and shape by the user into the LabView software, but no position measurement is carried out. Dedicated experiments were conducted to design the oscillation allowing the cancellation, or at least reduction, of COLIBRI's reactivity worth:

- Measurements of POLLEN reactivity worth axial profile by means of slow sample insertion and inverse kinetic calculations (Figure 16, left).
- Reactivity worth estimates of COLIBRI by inverse kinetic calculations of measurements.
- Calculation of POLLEN movement shapes with centre position at height of 800 mm in order to compensate COLIBRI, as used during this experimental campaign in Figure 16 (right).

A detailed workflow for estimating the dynamic reactivity worth of COLIBRI oscillations, and calculating the corresponding POLLEN movement shape is described in Appendix 6.4.

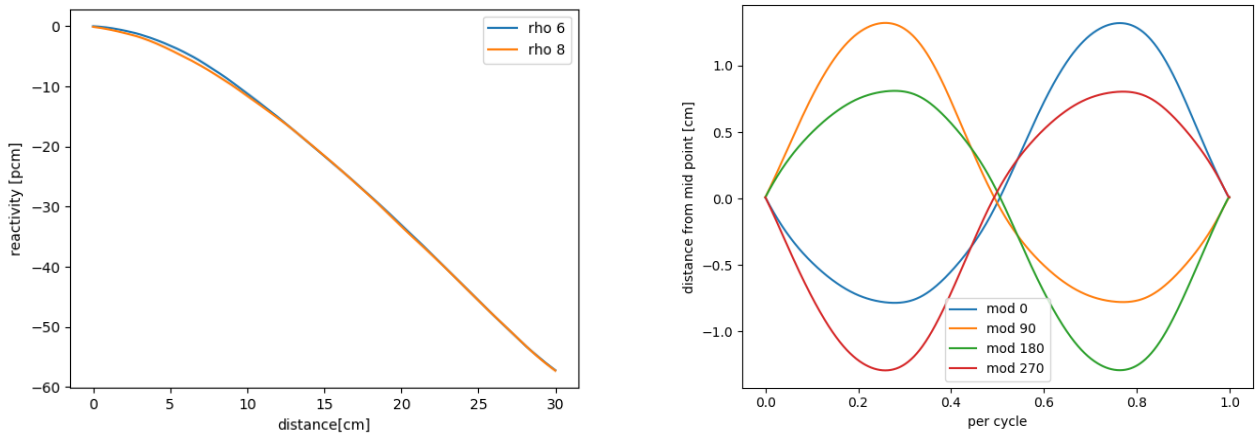

Figure 16 – On the left, reactivity worth vs. distance from the top of the guide tube of POLLEN sample mid-height, as measured by detectors 6 and 8. On the right, POLLEN displacement shapes with sample mid-height set at height 800 mm, which were used during this campaign.

3.3 Neutron detection instrumentation

3.3.1 Detectors

The detection instrumentation comprised the facility monitors, and different types of additional ex-core and in-core detectors, for a total of eighteen detectors of various sizes and sensitivities:

- Two safety monitors ^{235}U-coated fission chambers: Photonis CFUM21,
- Two operation monitors ^{10}B-coated compensated ionization chambers: Merlin-Gerin CC54,
- Two in-core small BF_3 proportional counters: Transcommerce International MN-1,
- Two in-core smaller BF_3 proportional counters: unknown brand and model,
- Two ex-core ^{3}He proportional counters: Canberra 12NH25/1F,
- Four ex-core large ^{235}U-coated fission chambers: Photonis CFUL01,
- One in-core ^{235}U-coated miniature fission chamber: Photonis CFUF34,
- **Three additional miniature scintillators**, following the developments at EPFL [4], [5].

The specification and location of each detector with respect to the core and COLIBRI are presented in Table 3 and Figure 17, and with respect to the MCNP model (coordinates and universes). For the majority of the detectors, the location was unchanged as compared to the second campaign – changes are highlighted in grey in Table 3, and discussed in this Section.

All detectors are based on prompt detection processes. Facility monitors (det. 1 to 4) are set at reference positions, as presented in the CROCUS benchmark [6] and models (all available on the ECCP). The specifications of other detectors, such as sensitive area and channels dimensions, are included in the Appendix 6.3, p. 32. On the axial plane, sensitive areas of all detectors are centered vertically at about core mid-height, but for detectors 9 and 10 (^{3}He PC), and 17 and 18 (scintillators). On the horizontal plane, detectors 11 to 14 (^{235}U FC) are set in the reflector at all four cardinal positions, including west, closest to COLIBRI. Detectors 5 to 8 (BF_3 PC) and 16 (scintillator) are set at positions within the lattice as presented in Figure 17: in the control rod guide tubes for the NW and SE ones (det. 5 and 16), and in aluminum channels for the other three (det. 6, 7 and 8). Detectors 9 and 10 (^{3}He PC) are set in a sheath of polyethylene and cadmium in order to cut their sensitivity to thermal neutrons (Cd), and enhance their sensitivity to fast neutrons (PE).

Table 3 – Detectors specifications with respect to the MCNP model coordinates. In italic, location coordinates within the lattice. Changes with respect to the 2nd campaign are highlighted in grey.

	Detector					Acquisition		Location (cm)			
#	Type	Brand	Model	Sensitive material	Sensitivity (n_{th}^{-1})	DAQ	Channel	East	North	Axial	MCNP
1	FC	Photonis	CFUM21	^{235}U coating	10^{-2}	V2495	96	+35.8	+8.7	-	u = 31
2	FC	Photonis	CFUM21	^{235}U coating	10^{-2}	V2495	97	-35.8	-8.7	-	u = 31
3	CIC	Merlin-Gerin	CC54	^{10}B coating	*3×10^{-14} A*	WaveSurfer10	3	-8.6	+36.35	-	u = 30
4	CIC	Merlin-Gerin	CC54	^{10}B coating	*3×10^{-14} A*	HDO6104A	3	+8.6	-36.35	-	u = 30
5	PC	-	-	$^{10}BF_3$ gas	10^{-2}	V2495	66	*16.0*	*-16.0*	50.0	-
6	PC	Trans. Int.	MN-1	$^{10}BF_3$ gas	10^{-2}	V2495	67	*27.7*	*10.2*	50.0	u = 21
7	PC	-	-	$^{10}BF_3$ gas	10^{-2}	V2495	68	*-21.8*	*21.8*	50.0	-
8	PC	Trans. Int.	MN-1	$^{10}BF_3$ gas	10^{-2}	V2495	69	*-27.7*	*-10.2*	50.0	u = 21
9	PC	Canberra	12NH25/1F	^{3}He gas	-	V2495	64	+52.3[1]	-25.0	57.0	-
10	PC	Canberra	12NH25/1F	^{3}He gas	-	V2495	65	-52.3[1]	+25.0	57.0	-
11	FC	Photonis	CFUL01	^{235}U coating	1	HDO6104A	1	-14.6	+29.5	50.5	-
12	FC	Photonis	CFUL01	^{235}U coating	1	HDO6104A	2	+32.4	+2.8	50.5	-
13	FC	Photonis	CFUL01	^{235}U coating	1	WaveSurfer10	1	-14.7	-29.5	50.5	-
14	FC	Photonis	CFUL01	^{235}U coating	1	WaveSurfer10	2	-33.1	-2.5	50.5	-
15	MFC	Photonis	CFUF34	^{235}U coating	10^{-3}	V2495	100	0	+11.5	50.0	-
16	Scint.	EPFL	-	^{6}Li doping	10^{-2}	V2495	70	16	-16	50.0	-
17	Scinti.	EPFL	-	^{6}Li doping	10^{-2}	V2495	71	34.3[2]	0	62.0	-
18	Scint.	EPFL	-	^{6}Li doping	10^{-2}	V2495	72	0	-7	80.0	-

[1] An error was made in the previous report, the value indicated here is valid for the second campaign as well.
[2] Nominal position, since the beam is moving with the movement of COLIBRI.

The three additional miniature neutron scintillation detectors were used to complement the array of detectors used in the 2nd experimental campaign. These are based on miniature ZnS(Ag):^{6}Li scintillator square screens of about 1 mm^2 and 0.28 mm thickness. Their light is guided to silicon photomultipliers via plastic optical fibers. They are operated in pulse mode. Their locations and specificities are as follows:

- Detector 16 was located at the NW control rod position inside a guide tube at core mid-plane. The detector was surrounded by a cadmium iris in the form of semi-circular plane, which can be rotated to expose the detector either to towards the COLIBRI oscillator or the core centre, towards the POLLEN oscillator.
- Detector 17 was located just behind the COLIBRI oscillator, glued to the aluminium beam (green on the left side of Figure 17) at an axial position of about 62.5 cm.
- Detector 18 was glued to the guide tube of the POLLEN oscillator at a height of 80.0 cm, corresponding to the POLLEN centre position.

Aside from these three additional detectors, the differences are as follows with respect to the 2nd campaign:

- Detector 16 (scintillator) replaced detector 5 (BF_3 PC) in the NW control rod guide tube;
- Because of issues with detector 7 (BF_3 PC), the equivalent detector 5 was used on the SE control rod guide tube, as its in-core position was deemed more useful;
- Detector 7 (BF_3 PC) was moved in an additional NW aluminum channel;
- Detector 15 (MFC) was shifted north from core center so as to leave the space to POLLEN.

The general uncertainty on detector position is ±1 mm, except for detectors 9 and 10 (^{3}He PC), for which it is ±5 mm.

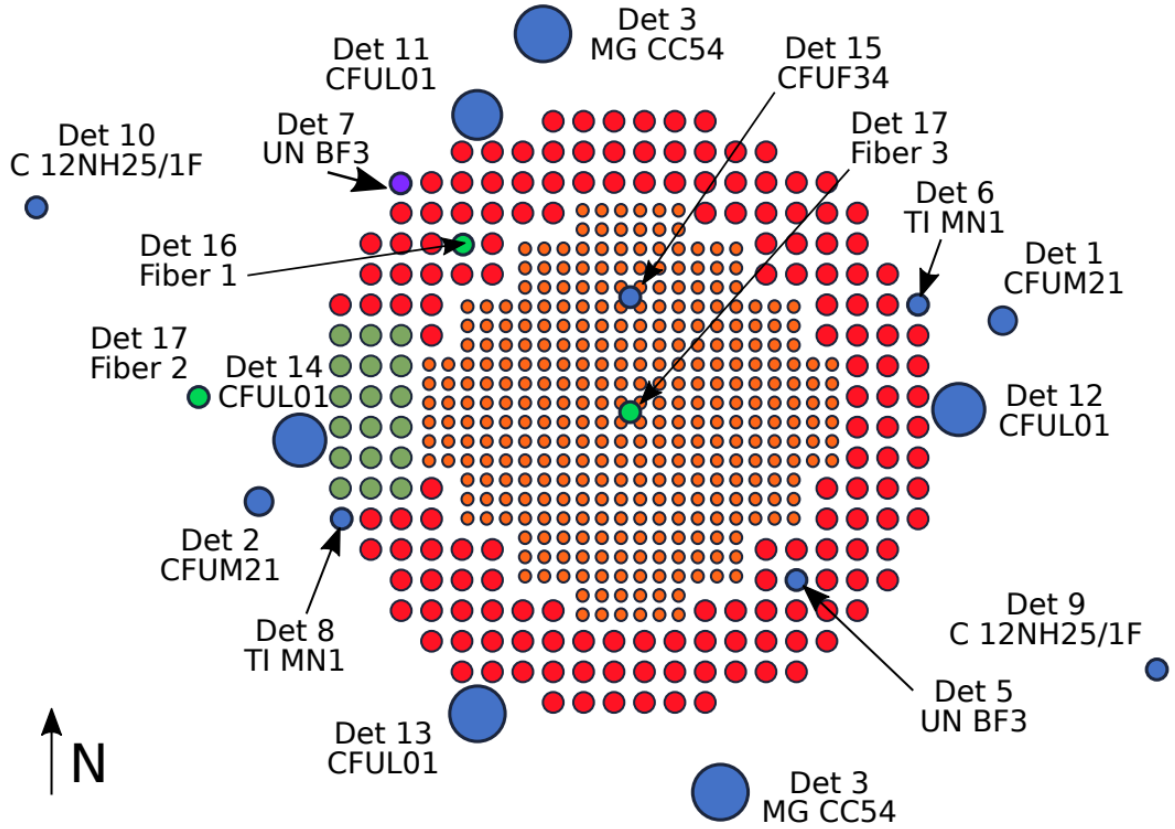

Figure 17 – Experimental setup of detectors.

3.3.2 Data acquisition systems

The operation ionization chambers and the large CFUL01 fission chambers were operated in current mode, whereas all the other detectors were operated in pulse mode. The detectors and their electronics were connected to three different data acquisition systems: two oscilloscopes for the current mode, and an FPGA programmable board for the pulse mode. All three systems were synchronized thanks to a start trigger, and recorded the inductive captor signal for allowing synchronization to the mechanical perturbation. In addition, the safety monitors were used in MCS mode for power monitoring using Canberra DSA-1000 data acquisition systems with the Genie2000 software.

3.3.2.1 Current mode acquisition systems

Two current mode acquisition systems were used for recording the CIC monitors (detectors 3 and 4), and the large CFUL01 fission chambers (detectors 11 to 14). They consist in in-house current amplifiers, which outputs are distributed between two Teledyne Lecroy oscilloscopes, namely a Wavesurfer 10, and an HDO6104A. The amplification scheme is depicted in Figure 18.

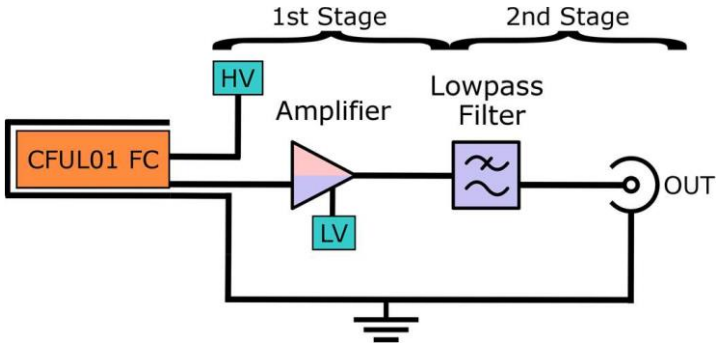

Figure 18 – Schematic of the in-house developed current amplifier connected to a typical large FC Photonis CFUL01, such as those used during the CROCUS campaign (detectors 11 to 14).

3.3.2.2 Pulse mode acquisition system

All pulse mode signals were recorded using an FPGA board from CAEN, namely the V2495. Detectors 5 to 10, i.e. all proportional counters, used CAEN low noise fast pre-amplification kits consisting in an A1427 preamplifier and an A1428 discriminator. The detector 15 miniature fission chamber used standard preamplifier (Tennelec 2025) and amplifier (Canberra 2022). The fiber detectors used the EPFL developed combinations of SiPM modules and pre-amplification and primary discrimination boards. Since the digital counting system was not yet fully validated at this point, the signal was additionally conditioned with a Gaussian amplifier (Canberra 2022) and a single channel analyzer (Canberra 2030), before being logged using the CAEN system.

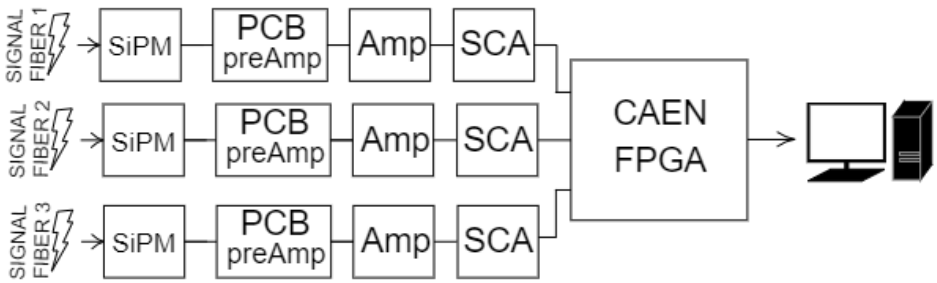

Figure 19 – Schematic of the fibers signal treatment and acquisition.

3.4 Experiments

The goal of the campaign was two-fold: repeatability, and spatial dependence enhancement. With respect to repeatability, although the reactor configuration was unchanged but for additional detectors and POLLEN, the core was fully unloaded and interfaces dismounted for another program (PETALE) between the 2nd and 3rd campaigns: the dependence on mechanical uncertainties should be accessible. A secondary goal was a better observation of the spatial dependence of noise by addition of POLLEN, synchronized to COLIBRI, as well as additional miniature scintillators located close to each perturbation. In addition, a detector sensitive to the angular dependence of flux (i.e. neutron current sensitive) was set in a control rod guide tube. All three perturbation cases were repeated in at least five measurement sets of 5000 s over the course of three different days.

Three types of experiments were carried out, namely static experiments, the reactivity characterization of POLLEN, and oscillation experiments:

- Static: determination of the critical configuration of extremal and nominal positions of rods within the oscillator, as well as corresponding signal in the detectors,
- POLLEN reactivity profile: slow insertion of the POLLEN Cd sample from totally withdrawn from the reactor, staying down for roughly 10 s, and then moving the Cd sample out of the reactor again
- Oscillation: long measurements of one setup only per perturbation, repeating a COLIBRI experiment of the 1st and 2nd campaigns. The above mentioned variations in setup include:
    - Used perturbation: COLIBRI only, POLLEN only, and with both POLLEN and COLIBRI (using different shapes for the POLLEN oscillator). The frequency was limited for all cases to 1 Hz. The oscillations of COLIBRI were limited to oscillating all 18 fuel rods with an amplitude of ±1.5 mm.
    - Cd iris position: exposing the fiber detector either towards core center (POLLEN) of towards East side (COLIBRI).

The reactor was operated with the water level, like the second campaign, in order to allow more in-core detectors by using both control rod guide tubes (see Figure 17). The global reactivity effect of the oscillations was compensated to follow a stable power. In practice, the oscillation was started first, then the reactor was stabilized in power with the water level before starting the measurements. The water level was updated along the experiments. The water temperature was controlled at 20.0 ± 0.1 °C. Following linearity tests, and thanks to the fast pulse mode electronics, the power was set around a higher power of 1 W. All oscillation experiments were acquired by all three acquisition systems, which were synchronized using a trigger. The duration of each measurement was maximized so as to reduce uncertainties as well, well above the first campaign. Waves at the surface of the water induced by oscillations were measured using the reactor instrumentation (INUS ultrasonic sensor).

38 experiments were carried out in total, which are listed in Table 4 (see next page) with their identification number. The table includes the oscillation specifications, as well as the final water level. The indicated values for water level oscillation correspond to the maximum range observed. The fuel rods oscillation is described in requested amplitude and frequency. For the static measurements, the rods position is indicated. The raw experimental data can be found on the Chalmers ftp server in the folder:

`/export/zh4/cortex/epfl/Experimental data/3rd CROCUS campaign/Raw_data`

The synchronized and pre-processed data can also be found on the Chalmers ftp server in the folder:

`/export/zh4/cortex/epfl/Experimental data/3rd CROCUS campaign/Pre-processed_data`

Measurements are distributed in subfolders (M{experiment number}), as well as corresponding synchronized COLIBRI cable position signals in a separate one. The files have the following naming convention:

`CROCUS_experiment number_E_detector number.txt`

“E” denotes the EPFL acquisition system. The inductive captor’s “detector number” is “pos”.

Table 4 – Experiments list with corresponding reactor state (including final position of water level, and water level oscillations' amplitude), orientation of detector 16, and oscillator specifications (used oscillator or static position of COLIBRI fuel rods, POLLEN shape, and ID).

Experiment				Reactor					Setup		
#	Type	Date	Start	Duration	Power	Water level	Water osc.	Det. 16 orientation	Oscillators (COLIBRI position)	POLLEN shape (Rate of movement)	Osc. ID
				s	mW	mm	mm	(SW/SE)			
1	Oscillation	04.03.21	18:03	1000	960	982.2	0.3	SE	COLIBRI	-	5
2	Oscillation	04.03.21	19:10	1000	1026	981.8	0.1	SE	Both	MOD_90	7
3	Static	05.03.21	10:31	1000	980	982.6	-	SE	0	-	-
4	Static	05.03.21	11:24	1000	900	982.1	-	SE	0	-	-
5	Oscillation	05.03.21	12:36	5000	980	982	0.2	SE	COLIBRI	-	9
6	Oscillation	05.03.21	14:47	5000	1000	982.1	0.2	SE	COLIBRI	-	9
7	Static	08.03.21	10:21	500	1000	982.0	-	SE	0	-	-
8	Oscillation	08.03.21	11:08	5000	970	982.2	0.2	SE	COLIBRI	-	11
9	Oscillation	08.03.21	12:42	5000	960	982.1	0.2	SE	COLIBRI	-	12
10	Oscillation	08.03.21	14:32	5000	990	982	0.2	SE	COLIBRI	-	14
11	Oscillation	08.03.21	16:20	500	1060	982.1	0.2	SE	Both	MOD_0	15
12	Oscillation	08.03.21	16:39	500	1000	981.8	0.2	SE	Both	MOD_90	15
13	Oscillation	08.03.21	16:53	500	970	981.8	0.2	SE	Both	MOD_180	15
14	Oscillation	08.03.21	17:07	500	950	982.1	0.2	SE	Both	MOD_270	15
15	Static	09.03.21	10:29	1000	960	983.1	-	SE	+1.5	-	-
16	Oscillation	09.03.21	12:06	5000	1080	981.6	0.2	SE	COLIBRI	-	17
17	Oscillation	09.03.21	14:43	5000	980	981.7	0.3	SE	Both	MOD_270	18
18	Oscillation	09.03.21	16:26	5000	990	982.1	0.2	SE	Both	MOD_270	19
19	Static	10.03.21	10:24	500	1010	981.1	-	SW	0	-	-
20	Oscillation	10.03.21	10:53	5000	940	982.2	0.4	SW	Both	MOD_270	20
21	Oscillation	10.03.21	13:29	5000	1010	981.9	0.2	SW	POLLEN	MOD_270	21
22	Oscillation	10.03.21	15:13	5000	970	982.1	0.4	SW	POLLEN	MOD_270	22
23	Reactivity	10.03.21	17:34	100	-	972.5	-	SW	-	(1 cm/s)	-
24	Reactivity	10.03.21	17:45	100	-	972.5	-	SW	-	(1 cm/s)	-
25	Oscillation	11.03.21	14:30	5000	1000	981.9	0.3	SW	POLLEN	MOD_270	23
26	Static	12.03.21	13:01	500	940	981.3	-	SW	-1.5	-	-
27	Oscillation	12.03.21	13:31	5000	1010	981.8	0.2	SW	COLIBRI	-	25
28	Oscillation	12.03.21	15:07	5000	970	981.6	0.2	SW	COLIBRI	-	26
29	Static	15.03.21	10:39	500	980	982.8	-	SW	+1.5	-	-
30	Oscillation	15.03.21	11:23	5000	1040	981.9	0.2	SW	Both	MOD_270	28
31	Oscillation	15.03.21	12:03	5000	960	982	0.2	SW	Both	MOD_270	29
32	Oscillation	15.03.21	15:03	5000	950	981.8	0.2	SW	Both	MOD_90	30
33	Static	16.03.21	10:00	500	950	981.4	-	SE	-1.5	-	-
34	Oscillation	16.03.21	12:08	5000	980	981.4	0.2	SE	Both	MOD_90	32
35	Oscillation	16.03.21	15:08	5000	990	982.0	0.1	SE	POLLEN	MOD_270	33
36	Oscillation	16.03.21	16:53	5000	1005	982.1	0.1	SE	POLLEN	MOD_270	34
37	Oscillation	17.03.21	09:05:30	5000	1010	982.3	0.3	SW	Both	MOD_270	36
38	Oscillation	17.03.21	11:13	5000	1006	982.1	0.2	SW	Both	MOD_270	37

4 Conclusion

In the framework of the CORTEX project, the work package 2 targets the generation of high-quality neutron noise experimental data for the subsequent validation of computers methods and models developed in work package 1.

In this aim, the third campaigns in the TUD AKR-2 and EPFL CROCUS zero power experimental reactors were successfully carried out in February and March 2021. It consisted in measurements in reference static states, and with mechanical perturbations arising from rotating and vibrating absorbers, and from vibrating fuel rods and a vibrating absorber, respectively. The present report documents the setups and experiments for each facility and perturbation type. The experimental time series have been made available to the members of the consortium through the Chalmers FTP server.

Following this report, the experimental results will be prepared and distributed to the members of the consortium in the form of an internal report containing PSD powers and phase for each experiment, perturbation, and detector.

5 References

[1] V. Lamirand, M. Hursin, A. Rais, S. Hübner, C. Lange, J. Pohlus, U. Paquee, C. Pohl, O. Pakari, and A. Laureau, “Experimental report of the 1st campaign at AKR-2 and CROCUS,” CORTEX Deliverable 2.1, 2018.

[2] V. Lamirand, A. Rais, S. Hübner, C. Lange, J. Pohlus, U. Paquee, C. Pohl, O. Pakari, P. Frajtag, D. Godat, M. Hursin, A. Laureau, G. Perret, C. Fiorina, and A. Pautz, “Neutron noise experiments in the AKR-2 and CROCUS reactors for the European project CORTEX,” *EPJ Web Conf.*, vol. 225, p. 04023, Jan. 2020.

[3] V. Lamirand, S. Hübner, O. Pakari, F. Vitullo, K. Ambrožič, A. Knospe, and A. Rais, “Experimental report of the 2nd campaign at AKR-2 and CROCUS,” CORTEX Deliverable 2.2, 2020.

[4] V. Lamirand, F. Vitullo, K. Ambrožič, O. Pakari, L. Braun, and D. Godat, “Development of fibre-based neutron scintillators,” CORTEX Deliverable 2.3 (D2.3), 2021.

[5] F. Vitullo, V. Lamirand, J.-B. Mosset, P. Frajtag, O. Pakari, G. Perret, and A. Pautz, “A mm 3 Fiber-Coupled Scintillator for In-Core Thermal Neutron Detection in CROCUS,” *IEEE Trans. Nucl. Sci.*, vol. 67, no. 4, pp. 625–635, Apr. 2020.

[6] U. Kasemeyer, R. Früh, J. M. Paratte, and R. Chawla, “Benchmark on Kinetic Parameters in the CROCUS Reactor,” in *International Reactor Physics Experiments Handbook (IRPhE)*, no. 4440, OECD, Ed. 2007, p. 94.

[7] S. Hübner, A. Knospe, M. Viebach, C. Lange, and A. Hurtado, “Experimental determination of the zero power transfer function of the AKR-2,” *Physor 2020*, 2020.

[8] J. Paratte, R. Chawla, and H. Akie, “A numerical neutronics benchmark study for inert matrix plutonium fuels in uranium dioxide and mixed plutonium-uranium dioxide environments,” *Prog. Nucl. …*, vol. 38, no. 3, pp. 335–342, 2001.

[9] A. Trkov, M. Ravnik, H. Wimmer, B. Glumac, and H. Bock, “Application of the rod-insertion method for control rod worth measurements in research reactors,” *Kerntechnik*, vol. 60, no. 5–6, pp. 255–261, 1995.

6 Appendices

6.1 AKR-2 reactor kinetic data

Table 5 – MCNP simulated precursor parameters [7]

Group of precursor	β_i	Std. dev.	λ_i in s^{-1}	Std. dev. in s^{-1}
1	0.00027	0.00001	0.01334	0.00001
2	0.00137	0.00002	0.03273	0.00001
3	0.00133	0.00002	0.12079	0.00001
4	0.00296	0.00003	0.30293	0.00001
5	0.00123	0.00002	0.85011	0.00001
6	0.00050	0.00001	2.85508	0.00003
Sum	0.00766	0.00004	-	-

6.2 AKR-2 reactor complete list of experiments

A complete list of all conducted experiments can be seen in the following Table 6. Measurements designated as S{number} designate static measurements. “Doublemode” means that the position signal of the linear motor axis is triggered two times or once in one oscillation.

Table 6 – Complete list of experiments

Designation	Date	Time	Type	Frequency (Hz)	Center position (cm)	Amplitude (cm)	Measurement duration (s)	Zipfile	BB posdata	Doublemode
S01	22.02.2021	09:49	-	0			600	20210222-messung_0Hz.zip		
M01	22.02.2021	10:08	AVS	0.1			2000	20210222-messung_AVS_0.1Hz.zip		No
M02	22.02.2021	10:50	AVS	2			2000	20210222-messung_AVS_2Hz.zip		No
M03	22.02.2021	11:39	AVS	10			2000	20210222-messung_AVS_10Hz.zip		No
S02	22.02.2021	12:27	-	0			600	20210222-messung_0Hz-2.zip		
M04	22.02.2021	12:45	VA	2	14.5	0.5	2000	20210222-messung_VA_2Hz.zip	2021-02-22-2Hz-1.txt	No
M05	22.02.2021	13:40	VA	10	14.5	0.5	2000	20210222-messung_VA_10Hz.zip	2021-02-22-10Hz-1.txt	No
M06	22.02.2021	14:25	VA	0.1	14.5	0.5	2000	20210222-messung_VA_0.1Hz.zip	2021-02-22-0.1Hz-1.txt	No
M07	22.02.2021	15:59	VA	0.1	14.5	0.5	2000	20210222-messung_VA_0.1Hz-2.zip		Yes
S03	23.02.2021	11:38	-	0	14.5		600	20210223-messung_0Hz.zip		
M08	23.02.2021	12:10	VA	0.1	14.5	0.5	2000	20210223-messung_VA_0.1Hz.zip	2021-02-23-0.1Hz.txt	Yes
M09	23.02.2021	12:52	VA	2	14.5	0.5	2000	20210223-messung_VA_2Hz.zip	2021-02-23-2Hz.txt	No
M10	23.02.2021	13:38	VA	10	14.5	0.5	2000	20210223-messung_VA_10Hz.zip	2021-02-23-10Hz.txt	No
S04	23.02.2021	14:25	-	0			600	20210223-messung_0Hz-2.zip		
M11	23.02.2021	14:45	AVS	0.1			2000	20210223-messung_AVS_0.1Hz.zip		No
M12	23.02.2021	15:26	AVS	2			2000	20210223-messung_AVS_2Hz.zip		No

Designation	Date	Time	Type	Frequency (Hz)	Center position (cm)	Amplitude (cm)	Measurement duration (s)	Zipfile	BB posdata	Doublemode
M13	23.02.2021	16:09	AVS	10			2000	20210223-messung_AVS_10Hz.zip		No
S05	24.02.2021	10:20	-	0			600	20210224-messung_0Hz.zip		
M14	24.02.2021	10:50	VA	1	10.5	2	2000	20210224-messung_VA_1Hz.zip	2021-02-24-1Hz.txt	No
M15	24.02.2021	11:47	VA	0.1	10.5	3	2000	20210224-messung_VA_0.1Hz.zip	2021-02-24-0.1Hz.txt	Yes
M16	24.02.2021	12:40	VA	2	10.5	3	2000	20210224-messung_VA_2Hz.zip	2021-02-24-2Hz.txt	No
S06	24.02.2021	13:26	-	0			600	20210224-messung_0Hz-2.zip		
M17	24.02.2021	13:54	VA	2	16	3	2000	20210224-messung_VA_2Hz-2.zip	2021-02-24-2Hz-2.txt	No
M18	24.02.2021	16:02	VA	0.1	16	3	2000	20210224-messung_VA_0.1Hz-2.zip	2021-02-24-0.1Hz-2.txt	Yes
S07	25.02.2021	09:44	-	0			600	20210225-messung_0Hz.zip		
M19	25.02.2021	10:08	VA	1	10.5	2	2000	20210225-messung_VA_1Hz.zip	2021-02-25-1Hz.txt	No
M20	25.02.2021	11:16	VA	0.1	10.5	3	2000	20210225-messung_VA_0.1Hz.zip	2021-02-25-0.1Hz.txt	Yes
M21	25.02.2021	12:01	VA	2	10.5	3	2000	20210225-messung_VA_2Hz.zip	2021-02-25-2Hz.txt	No
S08	25.02.2021	12:55	-	0			600	20210225-messung_0Hz-2.zip		
M22	25.02.2021	13:28	Both	2	14.5	0.5	2000	20210225-messung_Both_2Hz.zip	2021-02-25-2Hz-2.txt	No
M23	25.02.2021	14:19	Both	0.1	14.5	0.5	2000	20210225-messung_Both_0.1Hz.zip	2021-02-25-0.1Hz-2.txt	Yes
M24	25.02.2021	15:18	Both	2	16	3	2000	20210225-messung_Both_2Hz-2.zip	2021-02-25-2Hz-3.txt	No
M25	25.02.2021	16:14	VA	2	14.5	0.5	2000	20210225-messung_VA_2Hz-2.zip	2021-02-25-2Hz-4.txt	No

Designation	Date	Time	Type	Frequency (Hz)	Center position (cm)	Amplitude (cm)	Measurement duration (s)	Zipfile	BB posdata	Doublemode
S09	26.02.2021	10:00	-	0			600	20210226-messung_0Hz.zip		
M26	26.02.2021	10:38	Both	2	14.5	0.5	2000	20210226-messung_Both_2Hz.zip	2021-02-26-2Hz.txt	No
M27	26.02.2021	11:29	Both	0.1	14.5	0.5	2000	20210226-messung_Both_0.1Hz.zip	2021-02-26-0.1Hz.txt	Yes
M28	26.02.2021	12:23	Both	2	16	3	2000	20210226-messung_Both_2Hz-2.zip	2021-02-26-2Hz-2.txt	No
S10	26.02.2021	13:05	-	0			600	20210226-messung_0Hz-2.zip		
M29	26.02.2021	13:27	VA	2	16	3	2000	20210226-messung_VA_2Hz.zip	2021-02-26-2Hz-3.txt	No
M30	26.02.2021	14:23	VA	0.1	16	3	2000	20210226-messung_VA_0.1Hz.zip	2021-02-26-0.1Hz-2.txt	Yes
M31	26.02.2021	15:10	AVS	4			2000	20210226-messung_AVS_4Hz.zip		No
M32	26.02.2021	15:55	AVS	4			2000	20210226-messung_AVS_4Hz-2.zip		No
S11	04.03.2021	14:41	-	0			600	20210304-messung_0Hz.zip		
M33	04.03.2021	15:01	AVS	10			2000	20210304-messung_AVS_10Hz.zip		No
M34	04.03.2021	16:06	AVS	2			2000	20210304-messung_AVS_2Hz.zip		No
S12	04.03.2021	09:51	-	0			600	20210309-messung_0Hz.zip		
M35	09.03.2021	10:18	AVS	0.1			2000	20210309-messung_AVS_0.1Hz.zip		
M36	09.03.2021	11:11	VA	2	14.5	0.5	2000	20210309-messung_VA_2Hz.zip	2021-03-09-2Hz.txt	No
M37	09.03.2021	12:04	VA	10	14.5	0.5	2000	20210309-messung_VA_10Hz.zip	2021-03-09-10Hz.txt	No
M38	09.03.2021	12:55	VA	0.1	14.5	0.5	2000	20210309-messung_VA_0.1Hz.zip	2021-03-09-0.1Hz.txt	Yes

Designation	Date	Time	Type	Frequency (Hz)	Center position (cm)	Amplitude (cm)	Measurement duration (s)	Zipfile	BB posdata	Doublemode
S13	09.03.2021	13:37	-	0			600	20210309-messung_0Hz-2.zip		
M39	09.03.2021	14:05	VA	1	10.5	2	2000	20210309-messung_VA_1Hz.zip	2021-03-09-1Hz.txt	No
M40	09.03.2021	14:51	VA	2	10.5	3	2000	20210309-messung_VA_2Hz-2.zip	2021-03-09-2Hz-2.txt	No
M41	09.03.2021	15:46	VA	0.1	10.5	3	2000	20210309-messung_VA_0.1Hz-2.zip	2021-03-09-0.1Hz-2.txt	Yes
S14	10.03.2021	09:48	-	0			600	20210310-messung_0Hz.zip		
M42	10.03.2021	10:14	Both	2	14.5	0.5	2000	20210310-messung_Both_2Hz.zip	2021-03-10-2Hz.txt	No
M43	10.03.2021	11:10	Both	0.1	14.5	0.5	2000	20210310-messung_Both_0.1Hz.zip	2021-03-10-0.1Hz.txt	Yes
M44	10.03.2021	11:59	Both	2	16	3	2000	20210310-messung_Both_2Hz-2.zip	2021-03-10-2Hz-2.txt	No
S15	10.03.2021	12:45	-	0			600	20210310-messung_0Hz-2.zip		
M45	10.03.2021	13:40	AVS	4			2000	20210310-messung_AVS_4Hz.zip		
M46	10.03.2021	15:57	VA	2	16	3	2000	20210310-messung_VA_2Hz.zip	2021-03-10-2Hz-3.txt	No

6.3 Specifications of the detectors of the CROCUS campaign

6.3.1 Photonis CFUL01 fission chamber

The Photonis CFUL01 fission chamber consists in a large tube with a 1-g ^{235}U coating, the internals are described in Figure 20. During the experimental campaign, it was set first in a Faraday cage consisting in an aluminum tubing, and then inserted in a PMMA in-air experimental channel, all set vertically below the superior grid (see Figure 21).

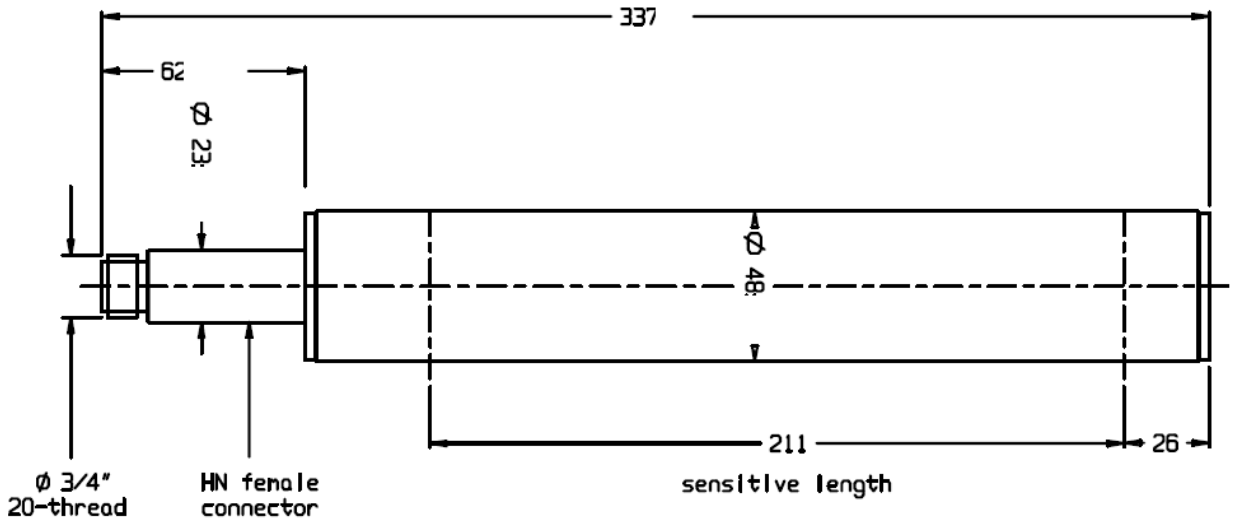

Figure 20 – Schematic of the Photonis CFUL01 fission chamber.

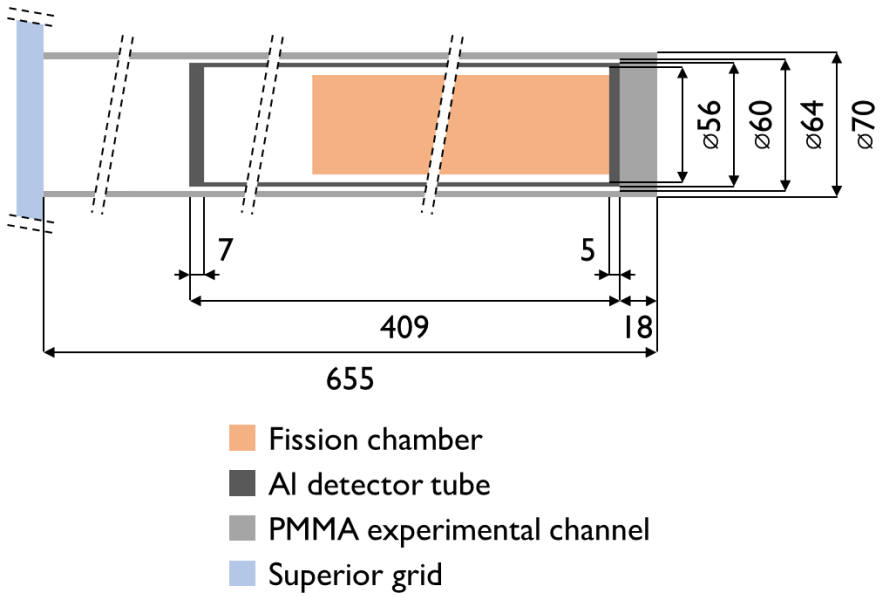

Figure 21 – Schematic of the fission chamber tube and in-air experimental channel with respect to the superior grid. NB: the channel is set vertically in-core, left side is top.

6.3.2 BF_3 proportional counters

Two types of BF_3 proportional counters were employed. Limited specification is available from the manufacturers for the Transcommerce International MN-1 detectors, and an x-ray image of the internals was carried out confirming them (see Figure 22). For the other and smaller BF_3 "grey" detectors, no information is available, neither series nor manufacturer. An x-ray image is considered, for now only the external dimensions are available. A summary of available information is presented in Table 7. The MN-1 PC were installed in in-air experimental channels lying at the bottom of the core, and whose diameter dimensions are presented in Figure 23. The others two "grey" detectors were set in the control rod guide tube (equivalent to an in-air U_{metal} cladding).

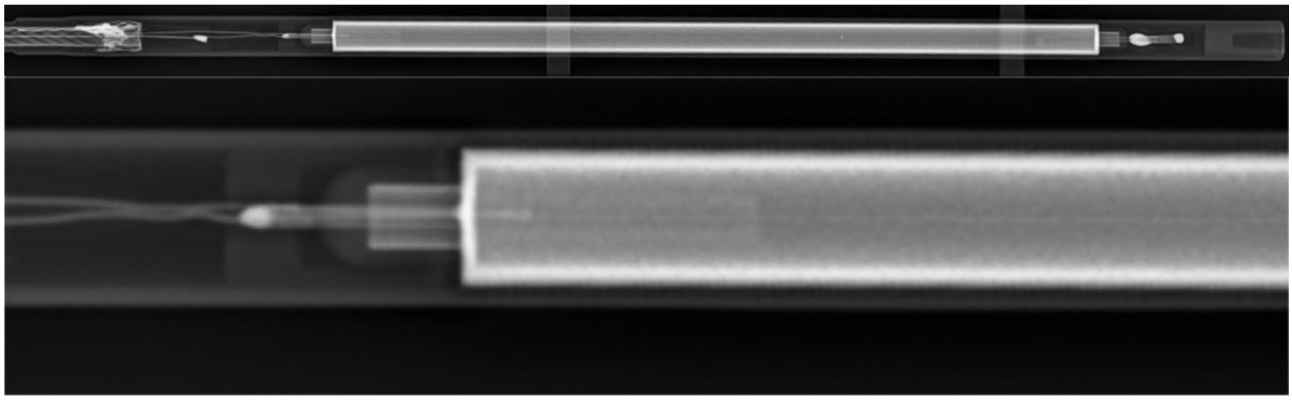

Figure 22 – X-ray image of a Transcommerce International MN-1 detector.

Table 7 – Specifications of the BF_3 proportional counters, from the supplier in the case of the Transcommerce International MN-1 detector, measured (casing) and estimated (active) for the "grey" smaller detector.

Supplier	Detector	Length (cm)			Diameter (cm)	
		Total	Al casing	Active	Al casing	Active
Trans. International	MN-1	25	18.4	12.7	0.75	0.63
Unknown	"Grey"	-	14.1	est. ~8.4	0.75	est.~0.63

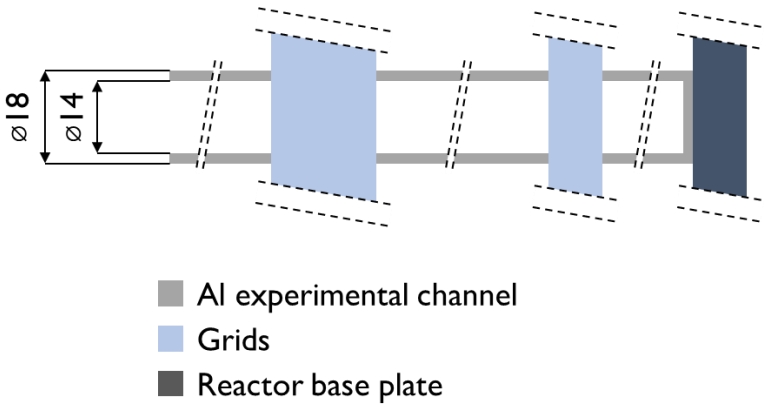

Figure 23 – Schematic of the in-air aluminum experimental channel used by the MN-1 BF_3 proportional counters, with respect to the grids and the reactor base plate. NB: the channel is set vertically in-core, left side is top.

6.3.3 *^{3}He proportional counters in Polyethylene and Cd sheats*

The ^{3}He detectors were set in a sheath of polyethylene and cadmium in order to cut their sensitivity to thermal neutrons (Cd), and enhance their sensitivity to fast neutrons (PE). All dimensions are indicated in Figure 24 and in Table 8.

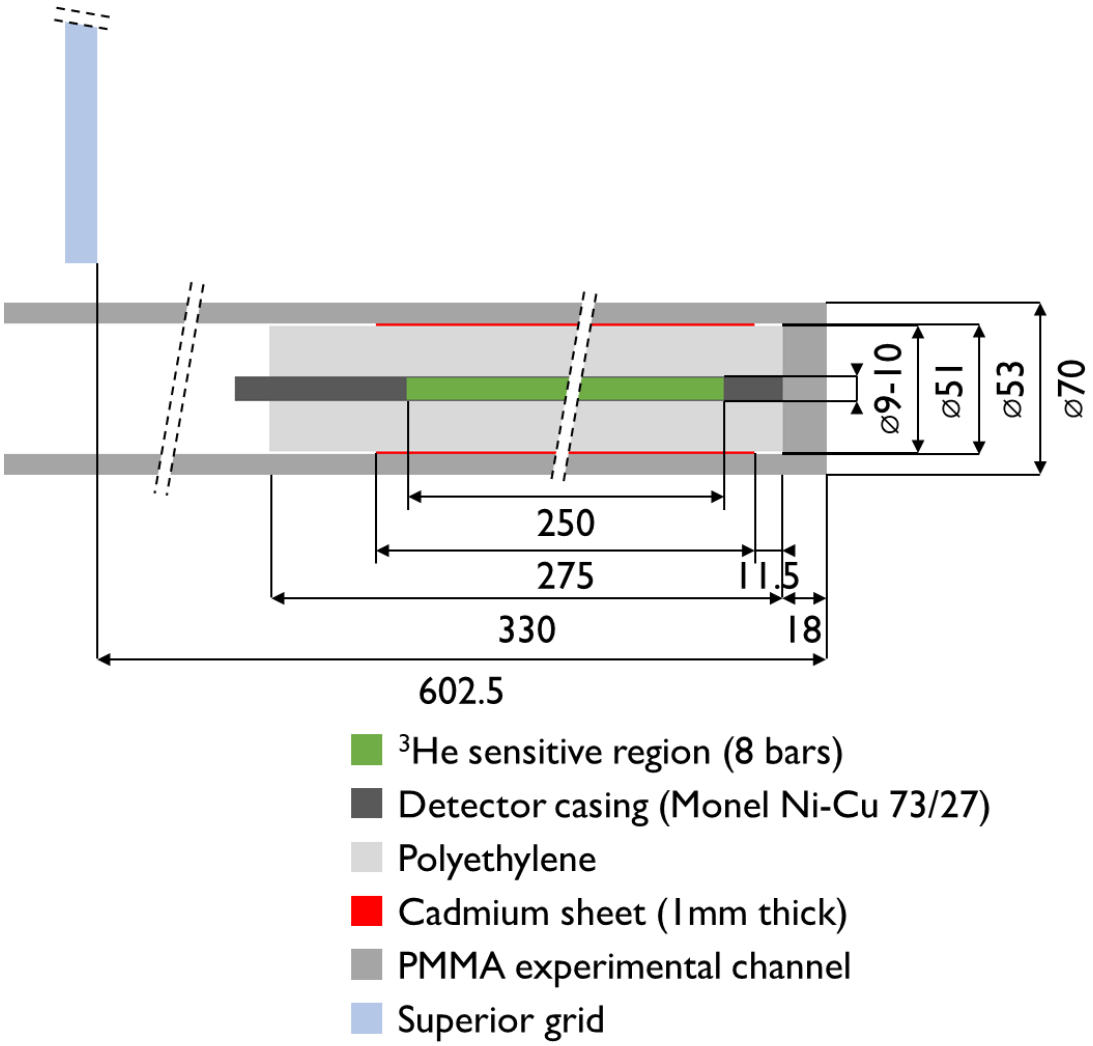

Figure 24 – Schematic of an ^{3}He detector set in its in-air experimental channel.

Table 8 – Specifications of the ^{3}He detectors.

Supplier	Model	Length (cm)		Diameter (cm)	
		Total	Active	Total	Active
Canberra	12NH25/1F	34,4	250	1.0	0.9

6.3.4 Photonis CFUF34 miniature fission chamber (TRAX)

The Photonis CFUF34 1-mg ^{235}U-coated miniature fission chamber is part of the CROCUS reactor system called TRAX. It allows translating radially and axially this watertight miniature detector along the slit between the two superior half-grids. It was set at core center during the whole measurement campaign. The schematic of the detector as provided by the supplier is presented in Figure 25.

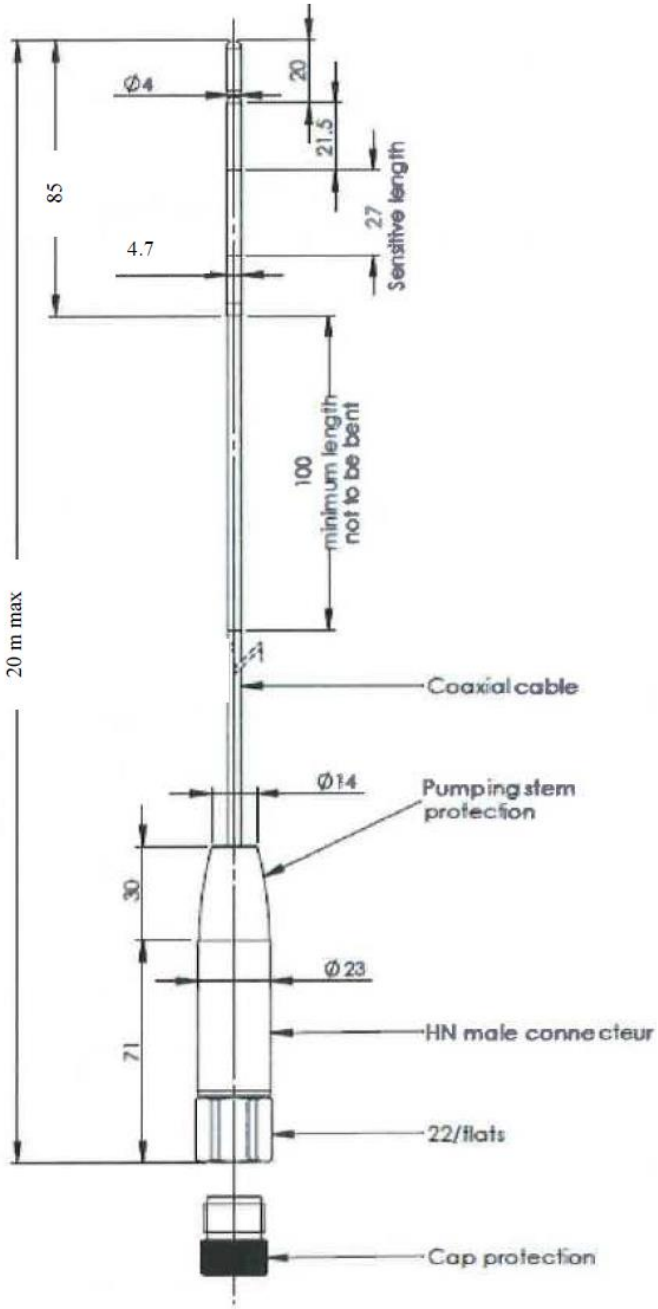

Figure 25 – Schematic of the Photonis CFUF34 miniature fission chamber. NB: the detector's side is at the bottom when set in-core.

6.4 Estimation of COLIBRI dynamic reactivity and calculation of POLLEN shapes for compensation

In order to make use of POLLEN to compensate the dynamic reactivity effects of COLIBRI, the workflow for calculating the movement shape of POLLEN goes as follows:

1. Noise measurement performed using COLIBRI only as a perturbation,
2. Application of inverse kinetic equations to the COLIBRI only experimental data for reactivity profile calculations, using CROCUS kinetic parameters [6], [8],
3. Averaging of reactivity over individual COLIBRI cycles,
4. POLLEN reactivity profile measurement by a “rod-insertion” technique [9], again applying the above mentioned evaluated CROCUS kinetic parameters,
5. Determination of suitable stable (stationary) position of POLLEN,
6. Calculation of POLLEN movement shape by applying its reactivity profile to the COLIBRI reactivity profile.

The movement shapes used during the experimental campaign were calculated based on the experimental data from the 2nd experimental campaign (considering point 1). Points 2 and 3 are explained in more detail below:

- Loading the pre-processed data of reference neutron detector (det. 12) and COLIBRI’s inductive captor, which is used for sectioning the experimental data (i.e., time series).
- Applying a Gaussian filter by convolution with a Gaussian kernel. In our particular case, a size of 11 samples (0.044s) was used.
- Calculating the neutron flux (i.e. detector signal) derivative by convolution with a kernel based on the five-point stencil numerical derivative formula,
- Calculating the initial concentration of neutron precursors by assuming stationary conditions; in our case, the mean of the detector signal is taken as an initial condition estimate,
- Calculating neutron precursor concentrations by integration from detector signal and initial estimate of neutron precursor concentrations,
- Calculating the mean and standard deviation of reactivity from each cycle using the inductive captor signal. A bias is removed, setting first and last reactivity of the cycle to 0, to remove reactivity induced by reactor control mechanisms. Since individual inductive captor pins were indistinguishable, separate estimates are made for each starting pin.

An example of reactivity analysis and reactivity estimate in time is displayed in Figure 26 (left), and the mean and standard deviation (colored area) of reactivity during a single COLIBRI cycle displayed in Figure 26 (right).

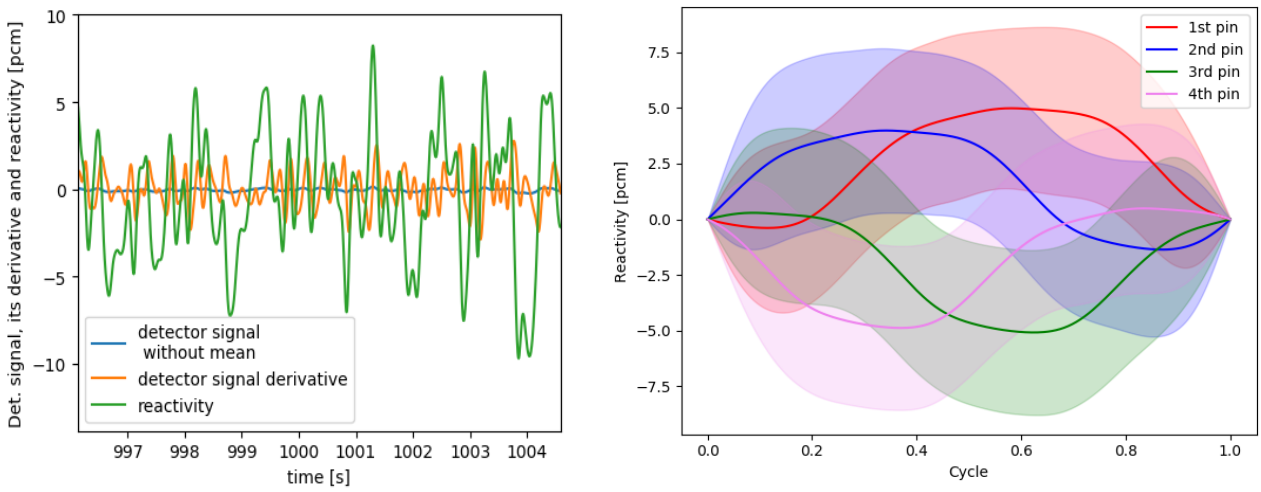

Figure 26 – On the left, detector signal, its derivative, and evaluated COLIBRI reactivity during experiment 8B of the 2nd campaign in CROCUS. On the right, mean and standard deviation of COLIBRI cycle reactivity, starting with a different inductive captor pin.